bioRxiv preprint doi: https://doi.org/10.1101/714048; this version posted July 24, 2019. The copyright holder for this preprint (which was not certified by peer review) is the author/funder, who has granted bioRxiv a license to display the preprint in perpetuity. It is made available under aCC-BY-NC-ND 4.0 International license.

Gene expression changes during female reproductive development in a colour polymorphic insect

B. Willink[1*†], M. C. Duryea[2], C. Wheat[3] and E. I. Svensson[1]

[1]Department of Biology, Evolutionary Ecology Unit, Ecology Building, Lund University, Lund 223-62, Sweden

[*]Corresponding author email: beatriz.willink@biol.lu.se

[†]Current address: School of Biology, University of Costa Rica, Sede Rodrigo Facio Brenes, San José, 11501-2060, Costa Rica

[2]Science Department, Great Basin College, Elko, Nevada, 89801, USA

[3]Department of Zoology, Stockholm University, Stockholm S-106 91, Sweden

Keywords: ecdysone, epistasis, heterochrony, pleiotropy, regulatory network, sexual dimorphism

bioRxiv preprint doi: https://doi.org/10.1101/714048; this version posted July 24, 2019. The copyright holder for this preprint (which was not certified by peer review) is the author/funder, who has granted bioRxiv a license to display the preprint in perpetuity. It is made available under aCC-BY-NC-ND 4.0 International license.

Abstract

Pleiotropy (multiple phenotypic effects of single genes) and epistasis (gene interaction) play key roles in the development of complex phenotypes and might be especially important in polymorphic taxa. The development of discrete and heritable sympatric phenotypic polymorphisms often emerges from major-effect genes that interact with other loci and have pleiotropic effects on multiple traits and physiological functions. We quantified gene expression changes during ontogenetic colour development in an insect (damselfly: *Ischnura elegans*) with three heritable female colour morphs, one which is a male mimic. Using transcriptome sequencing and *de novo* assembly, we demonstrate that all morphs show extensive downregulation of gene expression during early colour development. Morphs then become increasingly differentiated during sexual maturation and when developing adult colouration. These different ontogenetic trajectories arise because of the heterochronic development of the male-mimicking females, compared to other two female morphs. Many loci with regulatory functions in reproductive development are uniquely regulated in male-mimicking females, including upstream and downstream regulators of ecdysone signalling and transcription factors that influence insect sexual differentiation. Our study reveals extensive epistasis in the genomic architecture of *I. elegans* and suggest a central role for pleiotropy in shaping the developmental trajectories of the different morphs.

bioRxiv preprint doi: https://doi.org/10.1101/714048; this version posted July 24, 2019. The copyright holder for this preprint (which was not certified by peer review) is the author/funder, who has granted bioRxiv a license to display the preprint in perpetuity. It is made available under aCC-BY-NC-ND 4.0 International license.

Introduction

The role of epistasis (gene interaction) in shaping phenotypic variation and covariation has been discussed since the early days of the Modern Synthesis (Fisher 1930; Wright 1930; 1931), and still remains a contentious subject (Hill et al. 2008; Shao et al. 2008; Huang et al. 2012; Hemani et al. 2014; Mackay 2014; Wood et al. 2014). One way to investigate how gene interactions affect the development of phenotypic variants is to quantify the pleiotropic effects in gene expression profiles that arise as a result of allelic variance at single locus (e.g. Brem et al. 2005; Litvin et al. 2009). The number and function of differentially regulated genes between allelic variants can reveal epistatic interactions between the focal locus and other loci. Colour-polymorphic taxa are particularly suited for investigating such questions, as colour morphs typically differ in multiple physiological, developmental and life-history traits (Mckinnon and Pierotti 2010). The genetic basis of such heritable colour morphs is often quite simple and arises due to variation at one or a few loci with restricted recombination in between them (Joron et al. 2006; Thomas et al. 2008; Lamichhaney et al. 2016; Lindtke et al. 2017; Andrade et al. 2019). Pleiotropic effects of such major effect loci on the regulation of multiple other genes underlying morph differentiation and epistasis is likely to shape the development of such complex and co-adapted phenotypes.

There are two main mechanisms by which pervasive phenotypic differences can evolve in colour polymorphic systems with a relatively simple genetic architecture. Multiple loci involved in distinct pathways may be recruited into a chromosomal rearrangement, such as a chromosomal inversion with reduced recombination, effectively becoming physically linked as a 'supergene' (Kirkpatrick and Barton 2006; Schwander et al. 2014; Thompson and Jiggins 2014). Alternatively, genetic differentiation between morphs may arise from regulatory linkage (*sensu* West-Eberhard 2003) of a suite of co-selected traits underpinned by a polygenic architecture, whereby modularity and pleiotropy result from a few regulatory loci (Sinervo and Svensson 2002; Nijhout 2003; ten Tusscher and Hogeweg 2009). In this latter scenario, a colour-morph locus can evolve new

bioRxiv preprint doi: https://doi.org/10.1101/714048; this version posted July 24, 2019. The copyright holder for this preprint (which was not certified by peer review) is the author/funder, who has granted bioRxiv a license to display the preprint in perpetuity. It is made available under aCC-BY-NC-ND 4.0 International license.

regulatory functions at the top of a gene-regulatory network, in addition to already present developmental effects on multiple tissues (Monteiro and Podlaha 2009). Physiological epistasis – i.e. the dependency of a gene function on previously or simultaneously expressed gene products at other loci (Moore and Williams 2005) – would then underlie the pleiotropic effects of one or a few tightly linked colour-morph loci (Sinervo and Calsbeek 2003; ten Tusscher and Hogeweg 2009). Epistatic interactions arising from such a limited number of regulatory loci will emerge during the course of development, as phenotypic differences between adult morphs increase as they approach sexual maturation.

A substantial fraction of phenotypic evolution in the history of Metazoans has resulted from regulatory changes in the time, location and volume of interactions among gene products (Gerhart and Kirschner 2007). Many evolutionary novelties have arisen through a shift in the relative timing or rate of gene expression (e.g. Gomez et al. 2008; Albertson et al. 2010; Gunter et al. 2014), rather than due to the total disruption of previous interactions or the formation of entirely novel networks (Rebeiz et al. 2011). This phenomenon, known as heterochrony was historically considered to be a source of novel phenotypic variation between independently evolving lineages (Gould 1977; Reilly et al. 1997). However, variation in the timing of developmental events can also be important at the intraspecific level (Linksvayer and Wade 2005). A small but increasing body of evidence suggests that genetic control over regulatory networks can account for substantial phenotypic variation in several colour-polymorphic taxa (Kunte et al. 2014; Timmermans et al. 2014; Yassin et al. 2016; Takahashi et al. 2018). Heterochrony can produce large phenotypic changes but with only small genetic change (West-Eberhard 2003). These findings raise questions of how complex suites of physiological traits associated with colour polymorphisms emerge, and how variation in the timing and rate of developmental processes shape such profound intraspecific differences. By investigating how and when correlated trait differences between colour morphs arise during development, we can

bioRxiv preprint doi: https://doi.org/10.1101/714048; this version posted July 24, 2019. The copyright holder for this preprint (which was not certified by peer review) is the author/funder, who has granted bioRxiv a license to display the preprint in perpetuity. It is made available under aCC-BY-NC-ND 4.0 International license.

develop a better understanding of how epistasis and pleiotropy build up and shape different morphs within species.

Here, we investigated how changes in gene expression during the course of adult development differ among heritable female morphs in the trimorphic common bluetail damselfly (*Ischnura elegans*). This species, and several other species within the genus *Ischnura* have female-limited colour polymorphism that are maintained by frequency-dependent sexual conflict, in which common morphs suffer from reduced fitness due to excessive male mating harassment (Svensson et al. 2005; Gosden and Svensson 2009; Takahashi et al. 2010; Le Rouzic et al. 2015, Gering 2017). Female morphs differ in their ontogenetic trajectories of colour change and in suites of other phenotypic traits, including fecundity (Svensson and Abbott 2005; Willink et al. 2019), mating rates (Gosden and Svensson 2009), parasite resistance and tolerance (Willink and Svensson 2017), cold tolerance (Lancaster et al. 2017) and both larval (Abbott and Svensson 2005) and adult development times (Svensson et al. submitted). Thus, the colour locus (or a set of tightly linked loci) might be involved in epistatic interactions resulting in pleiotropic effects on the expression and timing of many other developmental processes.

We asked four major questions about the developmental regulation of gene expression in colour-developing females of three female morphs in *I. elegans*. First, at which point(s) in colour development do female morphs become different in their gene expression profiles? Second, which physiological processes characterise colour development across the female morphs of *I. elegans?* Third, which regulatory genes underlie these patterns? finally, are any physiological processes heterochronic between morphs with respect to colour development, and if so which ones? The answers to these questions will increase our understanding of how pleiotropy and epistasis shape the evolution of sex-limited polymorphisms.

bioRxiv preprint doi: https://doi.org/10.1101/714048; this version posted July 24, 2019. The copyright holder for this preprint (which was not certified by peer review) is the author/funder, who has granted bioRxiv a license to display the preprint in perpetuity. It is made available under aCC-BY-NC-ND 4.0 International license.

Methods

Study system

Females of the Common Bluetail damselfly (*Ischnura elegans*) occur in three heritable colour morphs whereas males are monomorphic (Fig. 1a). Previous studies using breeding experiments in controlled laboratory environments across multiple generations have revealed that colour morph development is governed by a single autosomal locus (or a set of tightly linked loci) with sex-limited expression to females (Cordero 1990; Sánchez-Guillén et al. 2005). These female morphs also undergo unique ontogenetic colouration changes, which are correlated with the onset of reproductive capacity and are not apparent in males (Cordero et al. 1998; Svensson et al. 2009; Willink et al. 2019). Female morphs differ in both their sexually mature (final) colour patterns as well as in the qualitative colour changes that are expressed during sexual development (Fig. 1). In *I. elegans*, these female morphs are typically referred to as 'Androchrome', 'Infuscans' and 'Infuscans-obsoleta'. To be consistent with previous publications (Willink and Svensson 2017), we hereafter refer to these three heritable female morphs, including both their immature and mature developmental phases, as A-, I- and O- females.

All three female morphs in *I. elegans* undergo pronounced ontogenetic changes in their colour pattern (Fig. 1b). Shortly after emergence from their last nymphal moult, A- and I-females exhibit a thoracic violet background colour with black antehumeral stripes. In A-females, the violet colour becomes turquoise-blue over post-emergence development, and therefore the final thoracic colour pattern of sexually mature A-females strikingly resembles the colour of males (Fig. 1). This adaptive colour change in A-females is consistent with male mimicry, for which there is experimental and observational evidence in species of *Ischnura* (Robertson 1985; Gosden and Svensson 2009; Gering 2017). In contrast, the violet thorax colour of I-females becomes greenish-brown in association with the onset of reproductive potential (Willink et al. 2019; Fig. 1b). Finally, O-females are also sexually dimorphic when sexually mature, but they do not exhibit distinct

bioRxiv preprint doi: https://doi.org/10.1101/714048; this version posted July 24, 2019. The copyright holder for this preprint (which was not certified by peer review) is the author/funder, who has granted bioRxiv a license to display the preprint in perpetuity. It is made available under aCC-BY-NC-ND 4.0 International license.

antehumeral stripes at any point in development and their thoracic colour changes from salmon-pink to brown (Cordero et al. 1998; Willink et al. 2019; Fig. 1b).

The two sexually dimorphic I- and O-females exhibit dramatic ontogenetic changes in the phenotypic expression of a blue patch on the eighth abdominal segment (Fig. 1b). This blue abdominal patch is initially present in sexually immature individuals of all three female morphs (Fig. 1b). However, in I- and O- females the blue patch subsequently becomes concealed by dark pigment over sexual development, whereas in males and the male-mimicking A-females, the blue colouration is instead retained during the entire course of sexual development (Henze et al. 2019; Fig. 1). All three female morphs therefore undergo ontogenetic colour changes over sexual development, but there are pronounced differences between A-females and the two heterochrome female morphs (I- and O-females). These colour changes occur continuously over the span of a few days (Svensson et al. submitted, Fig. 1b and S1). During this transitional period, individual females with intermediate phenotypes between the immature and mature developmental phases can be visually distinguished (Fig. 1b).

Fieldwork and sampling design

We sampled three females of each heritable colour morph at three stages of colour development, using the detailed description and classification of these colour stages by Cordero et al. (1998) and Svensson et al. (2009). The *immature* developmental phase was defined in all morphs by the presence of a contrasting blue colour patch in the distal portion of the abdomen, and for A-females by the simultaneous expression of the violet thoracic colouration. Females were classified to the *mature* developmental phase if they expressed the final colour phenotype of sexually mature individuals of their respective morph. Finally, *transitional* females expressed an intermediate phenotype between these two extremes. For I- and O- females these *transitional* individuals were identified by partial concealment of the blue patch with pigment, which results in a brownish-blue

bioRxiv preprint doi: https://doi.org/10.1101/714048; this version posted July 24, 2019. The copyright holder for this preprint (which was not certified by peer review) is the author/funder, who has granted bioRxiv a license to display the preprint in perpetuity. It is made available under aCC-BY-NC-ND 4.0 International license.

abdominal patch (Fig. 1b). *Transitional* A-females were characterised by a violet-turquoise thoracic colouration, which precedes the development of the final turquoise-blue background colour (Fig. 1b). All individuals in this study were collected in the field in southern Sweden during the summer of 2015 and from populations that form part of a long-term longitudinal study, in an area of approximately 40 x 40 Km^2 (TableS1; Svensson et al. 2005; Le Rouzic et al. 2015; Willink and Svensson 2017).

RNA sample preparation and sequencing

In addition to the 27 females sampled for the differential gene expression (DGE) analysis, an additional 58 *mature*-coloured females were sampled and used for the *de novo* transcriptome assembly below (Table S1). Field-caught individuals were bisected at the second abdominal segment and the two sections were preserved in RNAlater immediately following bisection and stored at -80 C within 1-4 h of capture. Samples were then shipped to the Beijing Genomics Institute (1/F, 16th Dai Fu Street, Tai Po Industrial Estate, Tai Po, Hong Kong) for extraction and sequencing. Total RNA was extracted using the Trizol LS Reagent (Life Technologies) following the manufacturer's instructions. RNAseq libraries were prepared for individual samples using the Illumina TruSeq kit with mRNA enrichment. Each sample was sequenced using 100 bp paired-end reads at a depth of 2 GB per sample on an Illumina HiSeq 2000. Raw data will be deposited at the National Center for Biotechnology Information (NBCI). Sample information and reads will be available through Biosample links and sequence read archives.

Transcriptome assembly and annotation

Raw reads were trimmed using Trimmomatic v.036 (Bolger et al. 2014) to remove adapter sequences and ambiguous nucleotides. We cropped the first 10 nucleotides of each read and trimmed regions of four nucleotides that had an average quality score below 20. Reads shorter than 25 nucleotides after trimming were discarded. All trimmed reads were pooled to assemble a

bioRxiv preprint doi: https://doi.org/10.1101/714048; this version posted July 24, 2019. The copyright holder for this preprint (which was not certified by peer review) is the author/funder, who has granted bioRxiv a license to display the preprint in perpetuity. It is made available under aCC-BY-NC-ND 4.0 International license.

reference transcriptome using Trinity v. 2.2.0 (Grabherr et al. 2011). Assembly quality was assessed by generating Ex50 estimates using scripts from the Trinity package (Haas et al. 2013), and by quantifying the ortholog hit ratio (OHR) (Vera et al. 2008; O'Neil et al. 2010; O'Neil and Emrich 2013). Ex50 estimates are generated by plotting the N50 of contigs for different expression quantiles, searching for the maximal N50 for regions capturing 70 – 90% of the expression data. OHR estimates were generated using the predicted protein set from the genome of the banded demoiselle damselfly, *Calopteryx splendens* (Csple_OGS_v1.0.faa; Ioannidis et al. 2017), then using blast (tblastn; Camacho et al. 2009) to search for the best hit of each protein in the *I. elegans* transcriptome assembly. OHR was then estimated by dividing the aligned length of an *I. elegans* transcript contig by the length of its orthologous *C. splendens* protein, wherein ratios of 1 indicate the full coverage of the contig for a given protein. The result was a single OHR estimate for each non-redundant protein from a related damselfly, the ortholog of which was found in the *I. elegans* transcriptome. The OHR distribution provides a detailed assessment of a transcriptome, indicating how well 1000's of genes have been assembled. Prior to analysis, redundancy due to isoforms and duplications in the *C. splendens* protein set was controlled by collapsing it by the longest protein isoform of each protein cluster group. This was based upon >90% amino acid identity using CD-HIT v4.5.4 (Li and Godzik 2006) with parameters used in making the UniRef90 database (Suzek et al. 2014). Annotation of the reference transcriptome was conducted using *blastx* v. 2.6.0+ with an e-value of 10e-5 against the National Center for Biotechnology Information (NCBI) non-redundant database (nr). Blast hits were then mapped to Gene Ontology (GO) terms using Blast2GO v. 4.1.9 (Conesa et al. 2005). If the blasted sequences returned more than a single hit, only the highest scoring hit was used in subsequent gene ontology (GO) enrichment analysis.

Data Pre-processing

Prior to the DGE analysis we used the CORSET algorithm (Davidson and Oshlack 2014) to reduce the number of spurious isoforms, which often arise during *de novo* transcriptome assemblies of non-

bioRxiv preprint doi: https://doi.org/10.1101/714048; this version posted July 24, 2019. The copyright holder for this preprint (which was not certified by peer review) is the author/funder, who has granted bioRxiv a license to display the preprint in perpetuity. It is made available under aCC-BY-NC-ND 4.0 International license.

model organisms due to sequencing artefacts. CORSET hierarchically clusters contigs based on shared reads and expression levels. In this case, clusters were based on the 27 samples to be used in our DGE analysis. The read counts are then summarised by these clusters, providing gene-level transcript abundances. Lowly expressed genes (i.e. with fewer than one read per million reads in at least three samples) were discarded at this stage and gene expression distributions were normalised via the weighted trimmed mean of M-values (TMM) method (Robinson and Oshlack 2010).

Differential gene expression analysis

DGE analyses were conducted using the packages *edgeR* (Robinson et al. 2010; McCarthy et al. 2012) and *limma* (Ritchie et al. 2015) in R v. 3.4.4 (R Core Team 2018), and were based on the workflow describe by (Law et al. 2016). In order to apply linear-based statistical modelling to the expression data, we estimated the mean-variance relationship in the log transcript counts per million (log-cpm), and incorporated this mean-variance trend into a precision weight for each normalised observation, using the voom method (Law et al. 2014; Liu et al. 2015). The advantage of this statistical approach, which estimates the mean-variance relationship instead of specifying a generating probabilistic distribution, is that it more appropriately controls for type I error rates when sample sizes are small and when sequencing depth varies between samples. In the *limma* pipeline these precision weights are then taken into account when fitting the linear models to the log-cpm gene expression data (Law et al. 2016). Empirical Bayes moderation was subsequently applied to these fitted models to more accurately estimate expression variability among genes and the 'robust' procedure was employed to allow variance outliers (Smyth 2004; Law et al. 2014; Phipson et al. 2016). Multiple testing across statistical contrasts was conducted using the "global" method, which is recommended when the number of differentially expressed (DE) genes is interpreted as a measure of the strength of a contrast (Smyth et al. 2018). The global method performs multiple testing adjustment across the entire set of contrasts and genes being tested. The P-value cut-off was

bioRxiv preprint doi: https://doi.org/10.1101/714048; this version posted July 24, 2019. The copyright holder for this preprint (which was not certified by peer review) is the author/funder, who has granted bioRxiv a license to display the preprint in perpetuity. It is made available under aCC-BY-NC-ND 4.0 International license.

adjusted according to Benjamini and Hochberg's false discovery rate (Benjamini and Hochberg 1995).

Our goal was to compare DGE across developmental stages and between the different colour morphs. Thus, we fitted a fully-factorial linear model including the fixed effects of female colour morphs, developmental phases and their interactions (~0 + Morph + Phase + Morph:Phase). With this model structure, the intercept is removed from the first factor (Morph), but kept in the second factor (Phase). Therefore, within each morph the immature phase is the intercept, and expression differences between groups can be compared by specifying a contrast matrix. Three types of comparisons are possible with the interaction term: (1) contrasts among morphs within each phase, (2) contrasts between subsequent phases within morphs and (3) and contrasts between developmental phases among colour morphs (full contrast matrix in Table S2). Because we sampled three females of each of three morphs and at each of three phases in colour development (27 females in total), developmental comparisons in (2) and (3) span one of two windows of colour development: *early* colour development, between the *immature* and *transitional* phases, and *late* colour development, between the *transitional* and *mature* phases. Our main focus in this study was on (3), because these contrasts represent the aspects of development that are regulated in opposite directions or with different magnitude among morphs. We used (2) to address the question of which genes are differentially expressed during the course of colour development and which are shared, either among morphs or between different developmental phases. We also used contrasts in (2) to identify the biological processes that are enriched during colour transitions for each female morph. These analyses are summarised in the next two sections. The results of contrasts among morphs within each phase (1) are presented in the Supporting Material (Fig. S2).

The ontogenetic colour changes are not of equal duration in all three morphs (Svensson et al. submitted). I- and O- females take a longer time to complete their colour maturation, compared to

bioRxiv preprint doi: https://doi.org/10.1101/714048; this version posted July 24, 2019. The copyright holder for this preprint (which was not certified by peer review) is the author/funder, who has granted bioRxiv a license to display the preprint in perpetuity. It is made available under aCC-BY-NC-ND 4.0 International license.

A-females (Fig. 1b and S1). Given our classification of developmental colour phases, this differential rate of colour change occurs only during *early* colour development, whereas *late* colour development is of a similar duration for all female morphs (Fig. 1b and S1). In spite of these differences in the time to transition among developmental phases, the *early* and *late* developmental windows represent a similar fraction of the full extent of colour changes that occur over development in each morph.

Correlations among subsets of differentially expressed genes

We used vector correlations to determine if developmental expression changes shared similar patterns across morphs for each colour transition (*early* and *late* colour development). Vector correlations have been more commonly used in studies of multivariate phenotypic evolution (Zelditch et al. 2012), but they are also useful to assess the similarity between estimated contrasts of gene expression across a set of multiple genes (Zinna et al. 2018). The correlation between two mean-centred vectors, each containing the estimated magnitude of expression differences between two experimental categories, is:

$$r_{vc} = \frac{|a \cdot b|}{\|a\| \times \|b\|} \quad (1)$$

where $a \cdot b$ is the dot product between the two vectors of statistical contrasts and $\|a\|$ and $\|b\|$ represent the magnitudes of vectors *a* and *b* respectively, and are given by the square root of the sum of squares of all contrast estimates. The gene vectors *a* and *b* in this study correspond to log-transformed coefficients estimated from the linear model and contrast matrix described above (Table S2). The vector correlation r_{vc} is equivalent to the Pearson correlation coefficient, such that values close to 1 indicate an almost perfect correlation between gene expression vectors, values close to 0 indicate no correlation and values close to -1 indicate nearly opposite regulation of gene expression between the two vectors.

bioRxiv preprint doi: https://doi.org/10.1101/714048; this version posted July 24, 2019. The copyright holder for this preprint (which was not certified by peer review) is the author/funder, who has granted bioRxiv a license to display the preprint in perpetuity. It is made available under aCC-BY-NC-ND 4.0 International license.

We followed the approach of Zinna et al. (2018) to determine if vector correlations between contrasts that have been considered significantly different from zero were particularly strong, compared to correlations between vectors of a random sample of genes, irrespective of the degree of statistical significance. This would indicate that those genes identified as significantly regulated across a period of colour development are also more similar (or dissimilar) in the direction of their regulation than a random gene vector of equal length. We defined in each case an experimental vector, for example, a vector containing all differentially expressed genes during *early* colour development that are shared between two female morphs. We then obtained an empirical distribution of vector correlations, drawn from 10 000 randomly sampled vectors of the same length as the experimental vector. We considered a correlation for the experimental vector as extreme when it fell outside the 95 percentile of correlations in equal-length random vectors.

Gene ontology enrichment analysis

To uncover the physiological changes that follow colour transitions in the different female morphs, we tested for significantly enriched GO terms in groups of developmentally regulated genes in comparison to the reference transcriptome, using the bioconductor package TopGO (Alexa and Rahnenfuhrer 2016) in R. For these analyses, we focused on contrasts between developmental colour phases within morphs (contrast group (2); Table S2). In the cases where multiple transcripts associated with a single gene (i.e. a Corset cluster) differed by at least one GO term (2 231 out of 30 134 mapped transcripts), all GO terms mapped to the different transcripts were pooled, and every unique term was assigned to the gene. Given that our interest was to explore how physiological processes change over development in the three female morphs, here we focused on biological process ontologies. The significance of enriched terms was tested using Fisher's exact test and the '*elim*' algorithm, in order to account for the hierarchical structure of gene ontologies (Alexa et al. 2006). With this algorithm, more general annotations are excluded for genes already counted as

bioRxiv preprint doi: https://doi.org/10.1101/714048; this version posted July 24, 2019. The copyright holder for this preprint (which was not certified by peer review) is the author/funder, who has granted bioRxiv a license to display the preprint in perpetuity. It is made available under aCC-BY-NC-ND 4.0 International license.

significantly enriched for a more specific GO term. GO terms with P-values < 0.01 were considered significantly enriched in the gene set of interest, compared to the reference transcriptome.

Colour development, heterochrony and female fecundity

Our recent findings of faster colour development in A-females (Svensson et al. submitted, Fig. 1b) and a higher number of differentially expressed genes during *late* colour development in this morph only (see Results) indicates that A-females reach their final developmental colour phase earlier than I- and O-females. This also suggests that this colour change might be decoupled from other developmental processes, including reproductive maturation. To test the idea that colour development could be faster (i.e. heterochronic) than most other developmental changes in A-females, we first compared *early* and *late* expression changes within each female morph, using the vector correlation approach described above. A-females reach their mature colour at about the same absolute age as I- and O- females develop their *transitional* phase (Svensson et al. submitted, Fig. 1b). If most other developmental changes proceed at similar rates in all female morphs, we would expect expression contrasts in *early* and *late* colour development to be more correlated in A-females than in the other two morphs, as in A-females these two developmental periods span a shorter absolute time. In contrast, if the fast colour changes of A-females indicates overall faster development, we would expect *early* and *late* expression contrasts to be as different in A-females as in I- and O-females, despite the shorter duration of *early* colour development in A-females.

Furthermore, if A-females accelerate their colour maturation in relationship to reproductive development, we expect that field-caught A-females in their final developmental colour phase would more often exhibit reproductive failure than I- and O-females, because at any given time a fraction of the mature-coloured A-females would still be sexually immature. Our fecundity data to test this prediction come from our surveys of 18 natural populations in Southern Sweden, which were visited frequently during the mating season (June to August) for 2-17 years, between 2001 and

bioRxiv preprint doi: https://doi.org/10.1101/714048; this version posted July 24, 2019. The copyright holder for this preprint (which was not certified by peer review) is the author/funder, who has granted bioRxiv a license to display the preprint in perpetuity. It is made available under aCC-BY-NC-ND 4.0 International license.

2017 (Svensson et al. 2005; Le Rouzic et al. 2015; Willink and Svensson 2017). During these visits, mating couples were collected in the field. Mated females were placed in individual plastic containers with moist filter paper for oviposition. After 72 h eggs were scanned at 1 200 dpi and subsequently counted using ImageJ (Schindelin et al. 2012).

In these surveys, mated females were classified by morph and developmental phase. However, *transitional* females were not classified as such, and before 2015 we did not distinguish between A- and I-females in the *immature* developmental phase (Fig. 1b). Therefore, we modelled the probability of reproductive failure only for the *immature* and *mature* developmental phases, and all data on *immature* A- and I-females come from the last three years of our population survey (2015-2017). We used a mixed-effect model fitted by MCMC in the *R* package MCMCglmm (Hadfield 2010) to test for a difference between morphs in the probability of reproductive failure, which we defined here as mated females that produced no viable eggs. We specified a binomial model with morph, developmental phase and their interaction as fixed effects. We also allowed for a random interaction between the population and season terms to affect the variance around the fixed effect estimates. All code to reproduce these analyses as well as the reproductive failure data will be uploaded to Dryad.

Results

Reference transcriptome

Using an extensive collection of RNA-Seq data, we assembled a transcriptome of 889,001 transcripts. Grouping transcripts by their expression levels and looking at those with the highest levels of expression in relation to their assembly lengths, a peak of transcript assembly length (N50) of nearly 3kb was found at expression levels containing 70-80% of transcripts (i.e. ExN50 ~ 3kb), suggesting sufficient data for a high quality assembly. We also estimated the OHR of our assembly by querying our assembly with the full protein set of the only published odonate genome, the

bioRxiv preprint doi: https://doi.org/10.1101/714048; this version posted July 24, 2019. The copyright holder for this preprint (which was not certified by peer review) is the author/funder, who has granted bioRxiv a license to display the preprint in perpetuity. It is made available under aCC-BY-NC-ND 4.0 International license.

375 banded demoiselle damselfly (*Calopteryx splendens*), which shared a common ancestor with *I. elegans* approximately 85 million years ago (the average from two dated phylogenies, 92 Ma in Thomas et al. 2013 and 79 million years in Waller and Svensson 2017). Of the 22,507 *C. splendens* proteins that were non-redundant, we found good hits (e-value less than 10e-5) for roughly 19,962, and of these, we found OHR of 0.7 and higher for nearly 70% (13,497; see Fig. S2 and Table S3).
380 Given the extensive divergence between the two taxa, the number of putative orthologs between species recovered is high and the strong skew towards high OHR values is indicative of a high quality transcriptome assembly.

General trends in early *colour development*

385 In all female morphs, *early* colour development, between the *immature* and *transitional* phases was characterised by extensive downregulation of gene expression. This was evidenced by comparisons between consecutive developmental phases and within morphs (contrast group (2); Table 1; Table S2). Across-the-board downregulation exceeded upregulation by a factor of more than 4, in O-females, to more than 25, in A-females (Table 1). Of all downregulated genes during *early* colour
390 development, 3 158 were shared by the three female morphs, whereas there were no upregulated genes shared by all morphs. The downregulated genes shared by all female morphs corresponded to ~ 62%, 75% and 67% of all downregulated genes in A-, I- and O- females, respectively. These genes were significantly enriched for biological processes involved in protein synthesis, transport and catabolism, energy metabolism, signal transduction, and cathecolamine biosynthesis (Table 2,
395 S4). Broadly shared downregulation of gene expression also resulted in highly correlated vectors of significantly regulated genes between all morph pairs (Fig. 2a).

General trends in late *colour development*

No single gene was either downregulated or upregulated in all female morphs during *late* colour
400 development. This absence of shared regulatory patterns was caused by the distinctiveness of A-

bioRxiv preprint doi: https://doi.org/10.1101/714048; this version posted July 24, 2019. The copyright holder for this preprint (which was not certified by peer review) is the author/funder, who has granted bioRxiv a license to display the preprint in perpetuity. It is made available under aCC-BY-NC-ND 4.0 International license.

females. There was a perfect negative correlation between A- and I-females in the regulation of genes that were differentially expressed in both morphs (Fig. 2a). Of 269 such genes, 164 were upregulated in I-females and downregulated in A-females and 105 exhibited the opposite regulatory pattern. There was also a negative correlation in the direction of regulation for the genes differentially expressed in A- and O-females, but this correlation was not particularly extreme (P = 0.14), as most genes, whether significant or not, exhibited opposite developmental contrasts during *late* colour development. In contrast, there were 66 genes with significant developmental regulation in both I and O-females and all of these genes were regulated in the same direction in both morphs (Fig. 2a). The biological processes enriched in the DE genes during *late* colour development were also markedly different between A-females and both I- and O-females. A-females upregulated genes enriched for functions in cell cycle progression, meiosis and the regulation of transcription, while downregulating multiple processes associated with energy metabolism (Table S6, S7). In contrast, both I- and O-females upregulated energy metabolic processes, while I-females downregulated lipid metabolisms and gene silencing and O-females downregulated genes participating in cell cycle progression, protein and RNA modification (Table S6, S7).

Colour development heterochrony and female fecundity

Unlike I- and O-females, which underwent a qualitative change in the direction of gene regulation at the onset of *late* colour development, regulation of gene expression was positively, although not extremely, correlated between *early* and *late* colour development in A-females (Fig. 2b). Such correlation between developmental periods in A-females was not extreme when compared to a random sample of expression contrasts drawn from equal-length gene vectors regardless of their significance level (P = 0.163; Fig. 2b). Nonetheless, downregulated genes during both *early* and *late* colour transitions in A-females were enriched for two shared biological processes, both associated with ATP biosynthesis (Table S4, S6). In contrast, no enriched biological processes were shared across development for either I- or O-females.

bioRxiv preprint doi: https://doi.org/10.1101/714048; this version posted July 24, 2019. The copyright holder for this preprint (which was not certified by peer review) is the author/funder, who has granted bioRxiv a license to display the preprint in perpetuity. It is made available under aCC-BY-NC-ND 4.0 International license.

We obtained data on reproductive failure of 5 247 (N_A = 3 336 , N_I = 1 667, N_O = 234) *mature*-coloured and 93 (N_A = 28 , N_I = 34, N_O = 21) *immature*-coloured females, all mated in the field. Across these three female morphs, *immature* developmental phases exhibited a nearly four-fold probability of reproductive failure compared to their *mature*-coloured counterparts (PMCMC < 0.001; Fig. 3). There were no differences in the rate of reproductive failure among the three female morphs in the immature phase (all PMCMC > 0.05; Fig. 3a). Among mature-colour individuals, reproductive failure was somewhat higher in A-females compared to I-females (PMCMC = 0.019; Fig. 3b), yet this difference was small relative to differences between mature and immature-coloured females (Fig 3).

Regulatory differentiation during colour development

There were more substantial morph differences in developmental regulation of gene expression during the second phase of colour development (contrast group (3) Table S2; Fig. 4). During this period, A-females became increasingly differentiated from both I- and O-females as revealed by the regulatory pattern of 856 genes (Fig. 4). Statistical contrasts for all these genes were of the same direction between A- and I-females and between A- and O-females.

To examine how epistatic effects of the colour-morph locus could mediate the differentiation of A-females, we queried the two subsets of genes which were differentially regulated between A- and both I- and O-females (contrast group (3); Table S2) for regulatory functions. First, we used the search term ‘juvenile hormone’ (JH), and ‘ecdysone’ (E), two major hormones involved in regulating insect reproduction and development (Simonet et al. 2004; Flatt et al. 2005). While we found no differentially regulated genes directly involved in JH metabolism, four genes related to ecdysone metabolism and signalling were upregulated in A-females compared I- and O-females during *late* colour development. To discern the potential functions of these genes, we used *blastx*

bioRxiv preprint doi: https://doi.org/10.1101/714048; this version posted July 24, 2019. The copyright holder for this preprint (which was not certified by peer review) is the author/funder, who has granted bioRxiv a license to display the preprint in perpetuity. It is made available under aCC-BY-NC-ND 4.0 International license.

against annotated proteins in the *Drosophila melanogaster* genome in FlyBase (Thurmond et al. 201). Three of these ecdysone-related genes were annotated to *D. melanogaster* genes in the *Halloween* group, which code for Cytochrome P450 enzymes that participate in ecdysone biosynthesis (Table 3, Fig. 5). The fourth gene was annotated as coding for the ecdysone-induced protein E74, a transcription factor that responds to concentrations of 20E in the ovary of *D. melanogaster* (Table 4; Fig. 6; Ables and Drummond-Barbosa 2010).

We further queried the gene sets differentiating A-females from both I- and O-females for regulatory functions, by identifying all genes in such subsets annotated with the GO term "regulation of transcription". This query revealed 18 genes, all differentially regulated during *late* colour development (Table 4). Most of these genes (~89%) increased in expression in A-females, while remaining relatively constant or decreasing in I- and O-females. We again used *blastx* against the *D. melanogaster* genome to examine the potential functions of these regulatory genes. We focus on the 13 genes that had good hits (e-value < 10e-5) against annotated proteins in SwissProt/TrEMBL (UniProt Consortium 2019). These genes comprised several transcription factors, including E74, a ribonucleoprotein and two proteins involved in histone acetylation (Table 4, Fig. 6).

Discussion

In this study, we investigated the regulatory changes that follow colour development in adult females of the trimorphic damselfly *I. elegans*. During the *early* phase of colour development, thousands of genes, underlying multiple metabolic processes, were significantly downregulated in all three female morphs (Table 1-2, S4). In striking contrast, upregulated genes were fewer and more idiosyncratic in function between morphs (Table 1, S5). This widespread downregulation of developmental gene expression resulted in strong correlations in the expression contrasts between the three different morphs (Fig. 2a). Soon after emergence from the final nymphal moult, gene

bioRxiv preprint doi: https://doi.org/10.1101/714048; this version posted July 24, 2019. The copyright holder for this preprint (which was not certified by peer review) is the author/funder, who has granted bioRxiv a license to display the preprint in perpetuity. It is made available under aCC-BY-NC-ND 4.0 International license.

expression is largely downregulated, potentially causing a slowdown in basic metabolism. The same pattern is present in holometabolous insects where more genes are downregulated than upregulated after pupation (e.g. Wang et al. 2010; Zheng et al. 2012), particularly in females (Graveley et al. 2011). Once energetically expensive tissues such as flight muscle have developed, resting metabolic rates also decline with age in adult insects (Hack 1997; Piiroinen et al. 2010; Niitepõld and Hanski 2013). Such metabolic cutback may contribute to delaying senescence (Sohal and Weindruch 1996).

Regulatory patterns during *early* colour development were also consistent with heterochronic colour development in A-females compared to the other two female morphs. Our recent work has shown that colour development is accelerated in the male-mimicking A-females compared to the two other female morphs (Svensson et al. submitted, Fig. S1). However, it it is still unclear whether the accelerated colour changes indicate that adult A-females develop overall faster or if they instead decouple their colour changes from other developmental processes. Disentangling between these two different alternatives is important to understand if ontogenetic colour changes in females act as signals of reproductive suitability, and to assess if the reliability of such signals varies among the different female morphs, which have alternative reproductive strategies (Willink et al. 2019).

We found that the expression contrasts during *early* and *late* colour development were negatively correlated in only I- and O-females (Fig. 2b). Some of the biological processes downregulated in all female morphs during *early* colour development, were also downregulated during *late* colour development in A-females (Table S4, S6). Moreover, mature A-females were more likely to exhibit reproductive failure than mature I-females, albeit this difference is relatively small (Fig. 3). A possible explanation for this morph difference is that A-females accelerate their reproductive development relative to other developmental changes, but such heterochrony comes at a fecundity cost, which sometimes results in reproductive failure. Across *Ischnura* species, developmental colour changes in heterochrome females (such as the I- and O-morphs) correlate with the onset of

bioRxiv preprint doi: https://doi.org/10.1101/714048; this version posted July 24, 2019. The copyright holder for this preprint (which was not certified by peer review) is the author/funder, who has granted bioRxiv a license to display the preprint in perpetuity. It is made available under aCC-BY-NC-ND 4.0 International license.

505 reproductive capacity and are used by males to identify suitable partners (Fincke 1987; Langenbach 1993; Takahashi and Watanabe 2011; Willink et al. 2019). Our data show that the accelerated ontogenetic colour changes in A-females of *I.elegans* might also affect their reproductive potential. In fact, A-females do also have lower average fecundity than both I- and O-females in the field (Svensson and Abbott 2005; Willink and Svensson 2017).

510

In adult females of *I. elegans*, most regulatory differences between morphs arise *late* in colour development (Fig. 4), when the colour differences between them are most apparent (Fig. 1b). During this period, A-females diverged from both I- and O-morphs in the expression pattern of 856 genes (Fig. 4b), while the overall expression patterns of I- and O-females remained largely similar
515 and positively correlated to each other (Fig. 2b). These results strongly suggest that the colour morph locus (or a set or tightly linked loci) interacts with hundreds of other loci during *late* colour development to produce the extensive phenotypic differentiation of the male-coloured morph. There are few well-documented examples of how epistatic interactions of a single or a few major loci influence the complex array of phenotypic traits that are associated with colour polymorphisms in
520 animals (Mckinnon and Pierotti 2010). In the side-blotched lizard (*Uta stansburiana*), a single locus segregating as a Mendelian factor with three alleles is the most parsimonious genetic model to explain throat-colour variation (Sinervo et al. 2001). The colour morph locus in *U. stansburiana* presumably interacts with the hypothalamic-pituitary-gonadal (HPG) hormonal axis, thereby regulating multiple loci involved in suites of different traits such as reproductive physiology,
525 immune function and territorial behaviour (Svensson et al. 2001; Sinervo and Svensson 2002; Sinervo and Calsbeek 2003). A simple genetic architecture of two loci was recently also demonstrated for colour polymorphic *Podarcis*-lizards (Andrade et al. 2019). Similarly in the ruff (*Philomachus pugnax*), a chromosomal inversion distinguishes a male-limited colour polymorphism associated with alternative mating-tactics, and in two of the three morphs this region has undergone

bioRxiv preprint doi: https://doi.org/10.1101/714048; this version posted July 24, 2019. The copyright holder for this preprint (which was not certified by peer review) is the author/funder, who has granted bioRxiv a license to display the preprint in perpetuity. It is made available under aCC-BY-NC-ND 4.0 International license.

deletions with putative cis-regulatory effects on genes involved in the metabolism of sex steroids, including testosterone (Lamichhaney et al. 2016).

The colour-morph locus in *I. elegans* likely interacts with numerous other genes via hormonal regulation. We found that three *I. elegans* genes with inferred roles in the ecdysone biosynthesis pathway were among the uniquely upregulated genes of A-females during *late* colour development. One of these genes was inferred to code for 20EMO, the enzyme that catalyses the conversion of E to 20E in the ovarian follicle and nurse cells of *D. melanogaster* (Table 3; Fig. 5a; Petryk et al. 2003; Rauschenbach et al. 2011). In insects, 20E induces ovarian cell development and is required in follicle cell differentiation and vitellogenesis (Swevers and Iatrou 2003; Simonet et al. 2004). The other two genes code for enzymes associated with upstream points in the ecdysone biosynthesis pathway (Table 3; Fig. 5b,c). Finally, an ecdysone responsive gene essential for oogenesis also showed upregulation during *late* colour development in only A-females (Table 4; Fig. 6a). In *D. melanogaster*, E74 responds to ecdysone titres to promote germline proliferation during early oogenesis, and is key for preventing germline degeneration during later stages of oogenesis (Ables and Drummond-Barbosa 2010).

The fact that both ecdysone biosynthesis and ecdysone-responsive genes are uniquely upregulated in A-females (Fig. 5, 6a) suggests that the colour morph locus might have pleiotropic effects via ecdysone signalling, regulating the timing of female reproductive development. Accelerated reproductive development in A-females during *late* colour development might partially compensate for their shorter period of colour transition, explaining why mature-coloured A-females are reproductively mature, just like I- and O-females, but have, on average, lower fecundity than these two other morphs (Svensson and Abbott 2005, Willink and Svensson 2017; Willink et al. 2019). This interpretation is also supported by the expression pattern of several other regulatory genes presumably involved in reproductive development (Table 4), all upregulated during *late* colour

bioRxiv preprint doi: https://doi.org/10.1101/714048; this version posted July 24, 2019. The copyright holder for this preprint (which was not certified by peer review) is the author/funder, who has granted bioRxiv a license to display the preprint in perpetuity. It is made available under aCC-BY-NC-ND 4.0 International license.

development of only A-females (Fig. 6b-f). For instance in *D. melanogaster*, a heterogeneous ribonucleoprotein (hnRNP) binds to poly(ADP-ribose) and this complex induces the expression of cadherin, which is in turn essential to maintain cell-cell adhesion during germline stem cell proliferation (Ji and Tulin 2012). hnRNPs can also be responsive to ecdysone levels through association with the protein on ecdysone puffs (PEP) (Amero et al. 1993). In *I. elegans*, both hnRNP and cadherin genes increase in expression during the late colour development of adult A-females, compared to both I- and O-females (Fig. 6b, S4a). Consistently, a gene coding for poly(ADP-ribose) glycohydrolase, the enzyme that degrades poly(ADP-ribose), was instead downregulated during *late* colour development in A-females compared to O-females (Fig. S4b), whereas PEP was upregulated (Fig. S4c).

In insects, changes in hormone titres or their intracellular response machinery can occur at critical periods causing qualitative developmental responses, such as those underlying the development of environmentally induced polyphenisms (Nijhout and Wheeler 1982; Nijhout 1999). Our results suggest a similar mechanism in the development in some of the pervasive phenotypic differences that distinguish A-females from the two other female morphs (heterochrome females). Instead of an environmental cue, the colour morph locus in *I. elegans*, might act at the top of a ecdysone-mediated hierarchy and gene cascade that governs the differential development of the three discrete adult female morphs.

The inferred functions of the regulatory genes uniquely expressed in A-females compared to I- and O-females are also consistent with the biological processes that characterised *late* colour development of A-females (Table 4, S6, S7). These regulatory genes have been implicated in cell cycle progression either in the ovary, regulating follicle and germ cell proliferation, or in other tissues of *D. melanogaster* (Table 4). During *late* colour development, the set of upregulated genes in A-females was significantly enriched for multiple processes necessary for cell cycle progression

bioRxiv preprint doi: https://doi.org/10.1101/714048; this version posted July 24, 2019. The copyright holder for this preprint (which was not certified by peer review) is the author/funder, who has granted bioRxiv a license to display the preprint in perpetuity. It is made available under aCC-BY-NC-ND 4.0 International license.

and division (Table S7). These results suggest that during adult development in *I. elegans* the colour-morph locus controls a regulatory cascade with pervasive effects on cell proliferation. These morph differences in the regulation of cell proliferation might occur primarily in the ovaries, as suggested by two of the biological processes enriched in the upregulated genes of A-females ("meoitic cell cycle" and "piRNA metabolic process"). While meiosis is a necessary step to produce gametes, piRNA protects the fidelity of genome transmission, by interacting with PIWI proteins to silence transpons in the germline (Malone et al. 2009). Accordingly, three out of four putative PIWI proteins in the *I. elegans* transcriptome were also upregulated in A-females during the *late* colour transition (Fig. S5).

The regulatory genes with unique expression patterns in A-females during *late* colour development also revealed a potential role of the colour-morph locus in inducing morph differentiation in somatic tissues of *I. elegans*. One of these genes mapped to *Dmrt* (Table 4) which is a gene family involved in sex determination and differentiation across animal taxa (e.g. Shen and Hodgkin 1988; Smith et al. 2009; Kato et al. 2011; Matson et al. 2011). This gene was upregulated in A-females compared to both I- and O-females. In somatic tissues of *D. melanogaster* the *Dmrt* gene, *doublesex* (*dsx*) integrates sexual identity, patterning and hormonal signals to induce the development of sexually dimorphic structures (Kopp 2012). Alternative splicing of *dsx* also underpins the development of male-mimicry in the female polymorphic butterfly *Papilio polytes* (Kunte et al. 2014). In the *I. elegans* congener *I. senegalensis*, heterochrome females are distinguished from both A-females and males in the expression pattern of a *dsx* isoform (Takahashi et al. 2018). *dsx* is therefore also a plausible regulator of the development of male mimicry in *I. elegans*, as it is differentially expressed between adult males and females (Chauhan et al. unpublished manuscript). However, we found no evidence of differential expression of *dsx* in *I. elegans* females, during the period of developmental colour changes (Fig. S6a). The *Dmrt* gene differentially expressed during *late* colour development in *I. elegans* lacks homology to the dimerization domain that characterises *dsx* (Bayrer

bioRxiv preprint doi: https://doi.org/10.1101/714048; this version posted July 24, 2019. The copyright holder for this preprint (which was not certified by peer review) is the author/funder, who has granted bioRxiv a license to display the preprint in perpetuity. It is made available under aCC-BY-NC-ND 4.0 International license.

et al. 2005), but as all other *Dmrt* genes it contains a DM DNA binding motif, which confers regulatory capacity over pseudopalindromic DNA targets (Zhu et al. 2000).

Holometabolous insects have multiple *Dmrt* genes (Wexler et al. 2014), and *I. elegans* has at least two (Fig. 6h, S6a). However, the functions of the *Dmrt* genes other than *dsx* are poorly known in insects, although these genes might also integrate sexual identity, spatial and temporal signals during sexual differentiation (Picard et al. 2015). While sex determination mechanisms are diverse across animal taxa, their downstream actions which result in sexual differentiation are typically more conserved and often rely on transcriptional regulation by the DM domain DNA binding motif (Zhu et al. 2000). In line with the possibility that this *Dmrt* gene may drive morph-specific development in *I. elegans*, we found that both a homeotic gene (Table 4, Fig. 6g) and two known targets of *dsx* (Fig. S6b-e) in *D. melanogaster* were also differentially expressed between male-mimicking A-females and both I- and O-females during *late* colour development.

In A-females, the expression of a homeotic gene annotated to *Sex combs reduced* (*Scr*) decreased as the expression of the *Dmrt* gene increased (Fig. 6g-h). Such epistatic interactions between *Dmrt* and homeotic genes have been described in *D. melanogaster* where both *dsx* and *Scr* are required for the proper localization of sexually dimorphic sex combs in male legs (Kopp 2011). Interestingly, we also found that three genes with similarity to *bric-á-brac* (*bab1/2*), a direct target of dsx in *D. melanogaster* (Christiansen et al. 2002) were also upregulated during late colour development in A-females (Fig. S6b-d). In *D. melanogaster*, *bab1/2* integrates *dsx* and homeotic inputs during the development of sexually dimorphic pigmentation (Kopp et al. 2000). Finally, the signalling peptide FMRFamide, another direct target of *dsx* in *D. melanogaster* (Luo et al. 2011), was also differentially regulated between A- and heterochrome females during late colour development. In *D. melanogaster*, FMRFamides modulate locomotory escape behaviour (Klose et al. 2010). In *I. elegans*, expression of the FMRFamide declines as the expression of the *Dmrt* gene increases (Fig.

bioRxiv preprint doi: https://doi.org/10.1101/714048; this version posted July 24, 2019. The copyright holder for this preprint (which was not certified by peer review) is the author/funder, who has granted bioRxiv a license to display the preprint in perpetuity. It is made available under aCC-BY-NC-ND 4.0 International license.

S6e). Together, these results suggests that conserved regulatory hierarchies downstream of sex determination might also partly regulate the developmental differentiation between the male-mimicking A-females and the two heterochrome I- and O-female morphs.

Conclusion

Here, we have investigated developmental regulation of gene expression during ontogenetic colour changes among heritable female colour morphs in *I. elegans*. Many regulatory changes occur shortly after the last larval moult (*early* colour development) and involve extensive downregulation of core metabolic processes in all female morphs. However, key regulatory differences between morphs emerge at a later ontogenetic stage (*late* colour development) when females develop their final colour patterns. These morph differences reflect heterochrony in colour development as male-mimicking females develop their final colouration faster, albeit at a fecundity cost. The regulatory genes that differentiate male mimics during *late* colour development suggested a unique temporal pattern of germ cell proliferation, presumably driven by ecdysone signalling that influence morph-specific differences in reproduction. Male-mimicking A-females also differ from the two other morphs in their expression of a *Dmrt* gene and its potential downstream targets. This suggests that the mechanisms behind somatic sexual differentiation and male mimicry might have a common underlying genomic and developmental basis. The colour-morph locus in *I. elegans* is therefore involved in many epistatic relationships with numerous other genes, presumably via hormonal pleiotropy. Our results provide insights on how pronounced phenotypic differences between these female morphs emerge during the course of development and reveal how epistasis and pleiotropy play key roles in the generation of complex and co-adapted phenotypes within this colour polymorphic species.

bioRxiv preprint doi: https://doi.org/10.1101/714048; this version posted July 24, 2019. The copyright holder for this preprint (which was not certified by peer review) is the author/funder, who has granted bioRxiv a license to display the preprint in perpetuity. It is made available under aCC-BY-NC-ND 4.0 International license.

References

Abbott, J., and E. I. Svensson. 2005. Phenotypic and genetic variation in emergence and development time of a trimorphic damselfly. J. Evol. Biol. 18:1464-1470.

Ables, E. T., and D. Drummond-Barbosa. 2010. The steroid hormone ecdysone functions with intrinsic chromatin remodeling factors to control female germline stem cells in *Drosophila*. Cell Stem Cell 7:581-592.

Ables, E. T., G. H. Hwang, D. S. Finger, T. D. Hinnant, and D. Drummond-Barbosa. 2016. A genetic mosaic screen reveals ecdysone-responsive genes regulating *Drosophila* oogenesis. G3-Genes Genom. Genet. 6:2629-2642.

Albertson, R. C., Y. L. Yan, T. A. Titus, E. Pisano, M. Vacchi, P. C. Yelick, H. W. Detrich, and J. H. Postlethwait. 2010. Molecular pedomorphism underlies craniofacial skeletal evolution in Antarctic notothenioid fishes. BMC Evol. Biol. 10:4.

Alexa, A., and J. Rahnenfuhrer. 2016. topGO: Enrichment analysis for gene ontology. R package version 2.30.1. URL: https://bioconductor.org/packages/release/bioc/html/topGO.html.

Alexa, A., J. Rahnenführer, and T. Lengauer. 2006. Improved scoring of functional groups from gene expression data by decorrelating GO graph structure. Bioinformatics 22:1600-1607.

Amero, S. A., M. J. Matunis, E. Matunis, J. W. Hockensmith, G. Raychaudhuri, and A. L. Beyer. 1993. A unique ribonucleoprotein complex assembles preferentially on ecdysone-responsive sites in *Drosophila melanogaster*. Mol. Cell. Biol. 13:5323-5330.

Andrade, P., C. Pinho, G. P. i de Lanuza, S. Afonso, J. Brejcha, C. J. Rubin, O. Wallerman, P. Pereira, S. J. Sabatino, A. Bellati, *et al*. 2019. Regulatory changes in pterin and carotenoid genes underlie balanced color polymorphisms in the wall lizard. Proc. Natl. Acad. Sci. U.S.A. 116:5633-5642.

Barmina, O., and A. Kopp. 2007. Sex-specific expression of a HOX gene associated with rapid morphological evolution. Dev. Biol. 311:277-286.

Bayrer, J. R., W. Zhang, and M. A. Weiss. 2005. Dimerization of *Doublesex* is mediated by a cryptic ubiquitin-associated domain fold: implications for sex-specific gene regulation. J. Biol. Chem. 280:32989-32996.

Benjamini, Y., and Y. Hochberg. 1995. Controlling the false discovery rate: a practical and powerful approach to multiple testing. J. Royal Stat. Soc. 57:289-300.

Bolger, A. M., M. Lohse, and B. Usadel. 2014. Trimmomatic: a flexible trimmer for Illumina sequence data. Bioinformatics 30:2114-2120.

Brem, R. B., J. D. Storey, J. Whittle, and L. Kruglyak. 2005. Genetic interactions between polymorphisms that affect gene expression in yeast. Nature 436:701-703.

Camacho, C., G. Coulouris, V. Avagyan, N. Ma, J. Papadopoulos, K. Bealer, and T. L. Madden. 2009. BLAST+: architecture and applications. BMC Bioinf. 10:421.

bioRxiv preprint doi: https://doi.org/10.1101/714048; this version posted July 24, 2019. The copyright holder for this preprint (which was not certified by peer review) is the author/funder, who has granted bioRxiv a license to display the preprint in perpetuity. It is made available under aCC-BY-NC-ND 4.0 International license.

Christiansen, A. E., E. L. Keisman, S. M. Ahmad, and B. S. Baker. 2002. Sex comes in from the cold: the integration of sex and pattern. Trends Genet. 18:510-516.

Conesa, A., S. Götz, J. M. Garcia-Gómez, J. Terol, M. Talón, and M. Robles. 2005. Blast2GO: a universal tool for annotation, visualization and analysis in functional genomics research. Bioinformatics 21:3674-3676.

Cordero, A. 1990. The inheritance of female polymorphism in the damselfly *Ischnura graellsii* (Rambur)(Odonata: Coenagrionidae). Heredity 64:341-346.

Cordero, A., S. S. Carbone, and C. Utzeri. 1998. Mating opportunities and mating costs are reduced in androchrome female damselflies, *Ischnura elegans* (Odonata). Anim. Behav. 55:185-197.

Cyran, S. A., A. M. Buchsbaum, K. L. Reddy, M. C. Lin, N. R. J. Glossop, P. E. Hardin, M. W. Young, R. V. Storti, and J. Blau. 2003. *vrille*, *Pdp1*, and *dClock* form a second feedback loop in the *Drosophila* circadian clock. Cell 112:329-341.

Davidson, N. M., and A. Oshlack. 2014. Corset: enabling differential gene expression analysis for de novo assembled transcriptomes. Genome Biol. 15:410.

Dobens, L. L., T. Hsu, V. Twombly, W. M. Gelbart, L. A. Raftery, and F. C. Kafatos. 1997. The *Drosophila* bunched gene is a homologue of the growth factor stimulated mammalian TSC-22 sequence and is required during oogenesis. Mech. Dev. 65:197-208.

Dobens, L. L., J. S. Peterson, J. Treisman, and L. A. Raftery. 2000. *Drosophila* bunched integrates opposing DPP and EGF signals to set the operculum boundary. Development 127:745-754.

Fincke, O. M. 1987. Female monogamy in the damselfly *Ischnura verticalis* Say (Zygoptera: Coenagrionidae). Odonatologica 16:129-143.

Fisher, R. A. 1930. The genetical theory of natural selection. Clarendon, Oxford, UK.

Flatt, T., M. Tu, and M. Tatar. 2005. Hormonal pleiotropy and the juvenile hormone regulation of *Drosophila* development and life history. Bioessays 27:999-1010.

Fox, D. T., and A. C. Spradling. 2009. The *Drosophila* hindgut lacks constitutively active adult stem cells but proliferates in response to tissue damage. Cell Stem Cell 5:290-297.

Gerhart, J., and M. Kirschner. 2007. The theory of facilitated variation. Proc. Natl. Acad. Sci. U.S.A. 104:8582-8589.

Gering, E. J. 2017. Male-mimicking females increase male-male interactions, and decrease male survival and condition in a female-polymorphic damselfly. Evolution 71:1390-1396.

Gomez, C., E. M. Özbudak, J. Wunderlich, D. Baumann, J. Lewis, and O. Pourquié. 2008. Control of segment number in vertebrate embryos. Nature 454:335-339.

Gosden, T. P., and E. I. Svensson. 2009. Density-dependent male mating harassment, female resistance, and male mimicry. Am. Nat. 173:709-721.

Gould, S. J. 1977. Ontogeny and phylogeny. Harvard University Press, Cambridge, USA.

bioRxiv preprint doi: https://doi.org/10.1101/714048; this version posted July 24, 2019. The copyright holder for this preprint (which was not certified by peer review) is the author/funder, who has granted bioRxiv a license to display the preprint in perpetuity. It is made available under aCC-BY-NC-ND 4.0 International license.

Grabherr, M. G., B. J. Haas, M. Yassour, J. Z. Levin, D. A. Thompson, I. Amit, X. Adiconis, L. Fan, R. Raychowdhury, Q. Zeng, and others. 2011. Full-length transcriptome assembly from RNA-Seq data without a reference genome. Nat. Biotechnol. 29:644-652.

Graveley, B. R., A. N. Brooks, J. W. Carlson, M. O. Duff, J. M. Landolin, L. Yang, C. G. Artieri, M. J. van Baren, N. Boley, B. W. Booth, and others. 2011. The developmental transcriptome of *Drosophila melanogaster*. Nature 471:473-479.

Gunawan, F., M. Arandjelovic, and D. Godt. 2013. The Maf factor Traffic jam both enables and inhibits collective cell migration in *Drosophila* oogenesis. Development 140:2808-2817.

Gunter, H. M., C. Koppermann, and A. Meyer. 2014. Revisiting de Beer's textbook example of heterochrony and jaw elongation in fish: calmodulin expression reflects heterochronic growth, and underlies morphological innovation in the jaws of belonoid fishes. Evodevo 5:8.

Haas, B. J., A. Papanicolaou, M. Yassour, M. Grabherr, P. D. Blood, J. Bowden, M. B. Couger, D. Eccles, B. Li, M. Lieber, and others. 2013. De novo transcript sequence reconstruction from RNA-seq using the Trinity platform for reference generation and analysis. Nat. Protoc. 8:1494-1512.

Hack, M. A. 1997. The effects of mass and age on standard metabolic rate in house crickets. Physiol. Entomol. 22:325-331.

Hadfield, J. D. 2010. MCMC methods for multi-response generalized linear mixed models: the MCMCglmm R package. J. Stat. Softw. 33:1-22.

He, Y., and R. Smith. 2009. Nuclear functions of heterogeneous nuclear ribonucleoproteins A/B. Cell. Mol. Life Sci. 66:1239-1256.

Hemani, G., K. Shakhbazov, H. Westra, T. Esko, A. K. Henders, A. F. McRae, J. Yang, G. Gibson, N. G. Martin, A. Metspalu, and others. 2014. Detection and replication of epistasis influencing transcription in humans. Nature 508:249-253.

Henze, M. J., O. Lind, B. D. Wilts, and A Kelber. 2019. Pterin-pigmented nanospheres create the colours of the polymorphic damselfly Ischnura elegans. J. Royal Soc. Interface 16:20180785.

Hill, W. G., M. E. Goddard, and P. M. Visscher. 2008. Data and theory point to mainly additive genetic variance for complex traits. PLos Genet. 4:e1000008.

Huang, W., S. Richards, M. A. Carbone, D. Zhu, R. R. H. Anholt, J. F. Ayroles, L. Duncan, K. W. Jordan, F. Lawrence, M. M. Magwire, and others. 2012. Epistasis dominates the genetic architecture of *Drosophila* quantitative traits. Proc. Natl. Acad. Sci. U.S.A. 109:15553-15559.

Ioannidis, P., F. A. Simao, R. M. Waterhouse, M. Manni, M. Seppey, H. M. Robertson, B. Misof, O. Niehuis, and E. M. Zdobnov. 2017. Genomic features of the damselfly *Calopteryx splendens* representing a sister clade to most insect orders. Genome Biol. Evol. 9:415-430.

Jennings, B., A. Preiss, C. Delidakis, and S. Bray. 1994. The Notch signalling pathway is required for Enhancer of split bHLH protein expression during neurogenesis in the *Drosophila* embryo. Development 120:3537-3548.

Ji, Y., and A. V. Tulin. 2012. Poly (ADP-ribose) controls DE-cadherin-dependent stem cell maintenance and oocyte localization. Nat. Commun. 3:760.

bioRxiv preprint doi: https://doi.org/10.1101/714048; this version posted July 24, 2019. The copyright holder for this preprint (which was not certified by peer review) is the author/funder, who has granted bioRxiv a license to display the preprint in perpetuity. It is made available under aCC-BY-NC-ND 4.0 International license.

Joron, M., R. Papa, M. Beltrán, N. Chamberlain, J. Mavárez, S. Baxter, M. Abanto, E. Bermingham, S. J. Humphray, J. Rogers, and others. 2006. A conserved supergene locus controls colour pattern diversity in *Heliconius* butterflies. PLoS Biol. 4:e303.

Kato, Y., K. Kobayashi, H. Watanabe, and T. Iguchi. 2011. Environmental sex determination in the branchiopod crustacean *Daphnia magna*: deep conservation of a *Doublesex* gene in the sex-determining pathway. PLoS Genet. 7:e1001345.

Kim, J., S. Lee, M. Hwang, S. Ko, C. Min, and J. Kim-Ha. 2009. Bunched specifically regulates α/β mushroom body neuronal cell proliferation during metamorphosis. Neuroscience 161:46-52.

Kirkpatrick, M., and N. H. Barton. 2006. Chromosome inversions, local adaptation, and speciation. Genetics 173:419-434.

Klose, M. K., J. S. Dason, H. L. Atwood, G. L. Boulianne, and A. J. Mercier. 2010. Peptide-induced modulation of synaptic transmission and escape response in *Drosophila* requires two G-protein-coupled receptors. J. Neurosci. 30:14724-14734.

Kopp, A. 2011. *Drosophila* sex combs as a model of evolutionary innovations. Evol. Dev. 13:504-522.

Kopp, A. 2012. Dmrt genes in the development and evolution of sexual dimorphism. Trends Genet. 28:175-184.

Kopp, A., I. Duncan, and S. B. Carroll. 2000. Genetic control and evolution of sexually dimorphic characters in *Drosophila*. Nature 408:553-559.

Kunte, K., W. Zhang, A. Tenger-Trolander, D. H. Palmer, A. Martin, R. D. Reed, S. P. Mullen, and M. R. Kronforst. 2014. Doublesex is a mimicry supergene. Nature 507:229-232.

Laherty, C. D., A. N. Billin, R. M. Lavinsky, G. S. Yochum, A. C. Bush, J.-M. Sun, T.-M. Mullen, J. R. Davie, D. W. Rose, C. K. Glass, and others. 1998. SAP30, a component of the mSin3 corepressor complex involved in N-CoR-mediated repression by specific transcription factors. Mol. Cell 2:33-42.

Lamichhaney, S., G. Fan, F. Widemo, U. Gunnarsson, D. S. Thalmann, M. P. Hoeppner, S. Kerje, U. Gustafson, C. Shi, H. Zhang, and others. 2016. Structural genomic changes underlie alternative reproductive strategies in the ruff (*Philomachus pugnax*). Nat. Genet. 48:84-88.

Lancaster, L. T., R. Y. Dudaniec, B. Hansson, and E. I. Svensson. 2017. Do group dynamics affect colour morph clines during a range shift? J. Evol. Biol. 30:728-737.

Langenbach, A. 1993. Time of color change in female *Ischnura pumilio* (Charpentier)(Zygoptera: Coenagrionidae). Odonatologica 22:469-477.

Law, C. W., M. Alhamdoosh, S. Su, G. K. Smyth, and M. E. Ritchie. 2016. RNA-seq analysis is easy as 1-2-3 with *limma*, *Glimma* and *edgeR*. F1000Research 5:1408.

Law, C. W., Y. Chen, W. Shi, and G. K. Smyth. 2014. voom: Precision weights unlock linear model analysis tools for RNA-seq read counts. Genome Biol. 15:R29.

bioRxiv preprint doi: https://doi.org/10.1101/714048; this version posted July 24, 2019. The copyright holder for this preprint (which was not certified by peer review) is the author/funder, who has granted bioRxiv a license to display the preprint in perpetuity. It is made available under aCC-BY-NC-ND 4.0 International license.

Le Rouzic, A., T. F. Hansen, T. P. Gosden, and E. I. Svensson. 2015. Evolutionary time-series analysis reveals the signature of frequency-dependent selection on a female mating polymorphism. Am. Nat. 185:E182-E196.

Li, W., and A. Godzik. 2006. Cd-hit: a fast program for clustering and comparing large sets of protein or nucleotide sequences. Bioinformatics 22:1658-1659.

Lindtke, D., K. Lucek, V. Soria-Carrasco, R. Villoutreix, T. E. Farkas, R. Riesch, S. R. Dennis, Z. Gompert, and P. Nosil. 2017. Long-term balancing selection on chromosomal variants associated with crypsis in a stick insect. Mol. Ecol. 26:6189-–6205.

Linksvayer, T. A., and M. J. Wade. 2005. The evolutionary origin and elaboration of sociality in the aculeate Hymenoptera: maternal effects, sib-social effects, and heterochrony. Q. Rev. Biol. 80:317-336.

Litvin, O., H. C. Causton, B.-J. Chen, and D. Pe'er. 2009. Modularity and interactions in the genetics of gene expression. Proc. Natl. Acad. Sci. U.S.A. 106:6441-6446.

Liu, R., A. Z. Holik, S. Su, N. Jansz, K. Chen, H. S. Leong, M. E. Blewitt, M.-L. Asselin-Labat, G. K. Smyth, and M. E. Ritchie. 2015. Why weight? Modelling sample and observational level variability improves power in RNA-seq analyses. Nucleic Acids Res. 43:e97.

Luo, S. D., G. W. Shi, and B. S. Baker. 2011. Direct targets of the *D. melanogaster* DSXF protein and the evolution of sexual development. Development 138:2761-2771.

Mackay, T. F. C. 2014. Epistasis and quantitative traits: using model organisms to study gene–gene interactions. Nat. Rev. Genet. 15:22-33.

Malone, C. D., J. Brennecke, M. Dus, A. Stark, W. R. McCombie, R. Sachidanandam, and G. J. Hannon. 2009. Specialized piRNA pathways act in germline and somatic tissues of the *Drosophila* ovary. Cell 137:522-535.

Matson, C. K., M. W. Murphy, A. L. Sarver, M. D. Griswold, V. J. Bardwell, and D. Zarkower. 2011. DMRT1 prevents female reprogramming in the postnatal mammalian testis. Nature 476:101-104.

McCarthy, D. J., Y. Chen, and G. K. Smyth. 2012. Differential expression analysis of multifactor RNA-Seq experiments with respect to biological variation. Nucleic Acids Res. 40:4288-4297.

Mckinnon, J. S., and M. E. R. Pierotti. 2010. Colour polymorphism and correlated characters: genetic mechanisms and evolution. Mol. Ecol. 19:5101-5125.

Monnier, V., M. Iché-Torres, M. Rera, V. Contremoulins, C. Guichard, N. Lalevée, H. Tricoire, and L. Perrin. 2012. dJun and Vri/dNFIL3 are major regulators of cardiac aging in *Drosophila*. PLoS Genet. 8:e1003081.

Monteiro, A., and O. Podlaha. 2009. Wings, horns, and butterfly eyespots: how do complex traits evolve? PLoS Biol. 7:e1000037.

Moore, J. H., and S. M. Williams. 2005. Traversing the conceptual divide between biological and statistical epistasis: systems biology and a more modern synthesis. Bioessays 27:637-646.

bioRxiv preprint doi: https://doi.org/10.1101/714048; this version posted July 24, 2019. The copyright holder for this preprint (which was not certified by peer review) is the author/funder, who has granted bioRxiv a license to display the preprint in perpetuity. It is made available under aCC-BY-NC-ND 4.0 International license.

Niitepõld, K., and I. Hanski. 2013. A long life in the fast lane: positive association between peak metabolic rate and lifespan in a butterfly. J. Exp. Biol. 216:1388-1397.

Nijhout, H. F. 1999. Control mechanisms of polyphenic development in insects: in polyphenic development, environmental factors alter some aspects of development in an orderly and predictable way. Bioscience 49:181-192.

Nijhout, H. F. 2003. Polymorphic mimicry in *Papilio dardanus*: mosaic dominance, big effects, and origins. Evol. Dev. 5:579-592.

Nijhout, H. F., and D. E. Wheeler. 1982. Juvenile hormone and the physiological basis of insect polymorphisms. Q. Rev. Biol. 57:109-133.

O'Neil, S. T., J. D. K. Dzurisin, R. D. Carmichael, N. F. Lobo, S. J. Emrich, and J. J. Hellmann. 2010. Population-level transcriptome sequencing of nonmodel organisms *Erynnis propertius* and *Papilio zelicaon*. BMC Genomics 11:310.

O'Neil, S. T., and S. J. Emrich. 2013. Assessing *De Novo* transcriptome assembly metrics for consistency and utility. BMC Genom. 14:465.

Ono, H., K. F. Rewitz, T. Shinoda, K. Itoyama, A. Petryk, R. Rybczynski, M. Jarcho, J. T. Warren, G. Marqués, M. J. Shimell, and others. 2006. *Spook* and *Spookier* code for stage-specific components of the ecdysone biosynthetic pathway in Diptera. Dev. Biol. 298:555-570.

Panchal, T., X. Chen, E. Alchits, Y. Oh, J. Poon, J. Kouptsova, F. A. Laski, and D. Godt. 2017. Specification and spatial arrangement of cells in the germline stem cell niche of the *Drosophila* ovary depend on the Maf transcription factor Traffic jam. PLoS Genet. 13:e1006790.

Petryk, A., J. T. Warren, G. Marqués, M. P. Jarcho, L. I. Gilbert, J. Kahler, J.-P. Parvy, Y. Li, C. Dauphin-Villemant, and M. B. O'Connor. 2003. *Shade* is the *Drosophila* P450 enzyme that mediates the hydroxylation of ecdysone to the steroid insect molting hormone 20-hydroxyecdysone. Proc. Natl. Acad. Sci. U.S.A. 100:13773-13778.

Phipson, B., S. Lee, I. J. Majewski, W. S. Alexander, and G. K. Smyth. 2016. Robust hyperparameter estimation protects against hypervariable genes and improves power to detect differential expression. Ann. Appl. Stat. 10:946-963.

Picard, M. A. L., C. Cosseau, G. Mouahid, D. Duval, C. Grunau, È. Toulza, J.-F. Allienne, and J. Boissier. 2015. The roles of *Dmrt* (Double sex/Male-abnormal-3 Related Transcription factor) genes in sex determination and differentiation mechanisms: Ubiquity and diversity across the animal kingdom. C.R. Biol. 338:451-462.

Piiroinen, S., L. Lindström, and A. Lyytinen. 2010. Resting metabolic rate can vary with age independently from body mass changes in the Colorado potato beetle, *Leptinotarsa decemlineata*. J. Insect Physiol. 56:277-282.

Rauschenbach, I. Y., E. Bogomolova, E. Karpova, N. Adonyeva, N. Faddeeva, P. Menshanov, and N. Gruntenko. 2011. Mechanisms of age-specific regulation of dopamine metabolism by juvenile hormone and 20-hydroxyecdysone in *Drosophila* females. J. Comp. Physiol. B 181:19-26.

bioRxiv preprint doi: https://doi.org/10.1101/714048; this version posted July 24, 2019. The copyright holder for this preprint (which was not certified by peer review) is the author/funder, who has granted bioRxiv a license to display the preprint in perpetuity. It is made available under aCC-BY-NC-ND 4.0 International license.

Rebeiz, M., N. Jikomes, V. A. Kassner, and S. B. Carroll. 2011. Evolutionary origin of a novel gene expression pattern through co-option of the latent activities of existing regulatory sequences. Proc. Natl. Acad. Sci. U.S.A. 108:10036-10043.

Reilly, S. M., E. O. Wiley, and D. J. Meinhardt. 1997. An integrative approach to heterochrony: the distinction between interspecific and intraspecific phenomena. Biol. J. Linn. Soc. 60:119-143.

Ritchie, M. E., B. Phipson, D. Wu, Y. Hu, C. W. Law, W. Shi, and G. K. Smyth. 2015. *limma* powers differential expression analyses for RNA-sequencing and microarray studies. Nucleic Acids Res. 43:e47.

Roberti, M., P. Fernandez-Silva, P. L. Polosa, E. Fernandez-Vizarra, F. Bruni, S. Deceglie, J. Montoya, M. N. Gadaleta, and P. Cantatore. 2005. In vitro transcription termination activity of the *Drosophila* mitochondrial DNA-binding protein DmTTF. Biochem. Biophys. Res. Commun. 331:357-362.

Robertson, H. M. 1985. Female dimorphism and mating behaviour in a damselfly, *Ischnura ramburi*: females mimicking males. Anim. Behav. 33:805-809.

Robinson, M. D., D. J. McCarthy, and G. K. Smyth. 2010. *edgeR*: a Bioconductor package for differential expression analysis of digital gene expression data. Bioinformatics 26:139-140.

Robinson, M. D., and A. Oshlack. 2010. A scaling normalization method for differential expression analysis of RNA-seq data. Genome Biol. 11:R25.

Sánchez-Guillén, R. A., H. Van Gossum, and A. Cordero Rivera. 2005. Hybridization and the inheritance of female color polymorphism in two ischnurid damselflies (Odonata: Coenagrionidae). Biol. J. Linn. Soc. 85:471-481.

Schindelin, J., I. Arganda-Carreras, E. Frise, V. Kaynig, M. Longair, T. Pietzsch, S. Preibisch, C. Rueden, S. Saalfeld, B. Schmid, and others. 2012. Fiji: an open-source platform for biological-image analysis. Nat. Methods 9:676-682.

Schwander, T., R. Libbrecht, and L. Keller. 2014. Supergenes and complex phenotypes. Curr. Biol. 24:R288-R294.

Scott, E. K., T. Lee, and L. Luo. 2001. *enok* encodes a *Drosophila* putative histone acetyltransferase required for mushroom body neuroblast proliferation. Curr. Biol. 11:99-104.

Shao, H., L. C. Burrage, D. S. Sinasac, A. E. Hill, S. R. Ernest, W. O'Brien, H. Courtland, K. J. Jepsen, A. Kirby, E. J. Kulbokas, and others. 2008. Genetic architecture of complex traits: large phenotypic effects and pervasive epistasis. Proc. Natl. Acad. Sci. U.S.A. 105:19910-19914.

Shen, M. M., and J. Hodgkin. 1988. *mab-3*, a gene required for sex-specific yolk protein expression and a male-specific lineage in *C. elegans*. Cell 54:1019-1031.

Simonet, G., J. Poels, I. Claeys, T. Van Loy, V. Franssens, A. De Loof, and J. V. Broeck. 2004. Neuroendocrinological and molecular aspects of insect reproduction. J. Neuroendocrinol. 16:649-659.

Sinervo, B., C. Bleay, and C. Adamopoulou. 2001. Social causes of correlational selection and the resolution of a heritable throat color polymorphism in a lizard. Evolution 55:2040-2052.

bioRxiv preprint doi: https://doi.org/10.1101/714048; this version posted July 24, 2019. The copyright holder for this preprint (which was not certified by peer review) is the author/funder, who has granted bioRxiv a license to display the preprint in perpetuity. It is made available under aCC-BY-NC-ND 4.0 International license.

Sinervo, B., and R. Calsbeek. 2003. Physiological epistasis, ontogenetic conflict and natural selection on physiology and life history. Integr. Comp. Biol. 43:419-430.

Sinervo, B., and E. Svensson. 2002. Correlational selection and the evolution of genomic architecture. Heredity 89:329-338.

Smith, C. A., K. N. Roeszler, T. Ohnesorg, D. M. Cummins, P. G. Farlie, T. J. Doran, and A. H. Sinclair. 2009. The avian Z-linked gene DMRT1 is required for male sex determination in the chicken. Nature 461:267-271.

Smyth, G. K. 2004. Linear models and empirical bayes methods for assessing differential expression in microarray experiments. Stat. Appl. Genet. Mol. Biol. 3:1-25.

Smyth, G. K., M. Ritchie, N. Thorne, J. Wettenhall, W. Shi, and Y. Hu. 2018. limma:linear models for microarray and RNA-Seq data user's guide. The Walter and Eliza Hall Institute of Medical Research. URL: http://bioconductor.org/packages/release/bioc/html/limma.html.

Sohal, R. S., and R. Weindruch. 1996. Oxidative stress, caloric restriction, and aging. Science 273:59-63.

Suzek, B. E., Y. Wang, H. Huang, P. B. McGarvey, C. H. Wu, and U. Consortium. 2014. UniRef clusters: a comprehensive and scalable alternative for improving sequence similarity searches. Bioinformatics 31:926-932.

Svensson, E., B. Sinervo, and T. Comendant. 2001. Density-dependent competition and selection on immune function in genetic lizard morphs. Proc. Natl. Acad. Sci. U.S.A. 98:12561-12565.

Svensson, E. I., and J. Abbott. 2005. Evolutionary dynamics and population biology of a polymorphic insect. J. Evol. Biol. 18:1503-1514.

Svensson, E. I., J. Abbott, and R. Härdling. 2005. Female polymorphism, frequency dependence, and rapid evolutionary dynamics in natural populations. Am. Nat. 165:567-576.

Svensson, E. I., J. K. Abbott, T. P. Gosden, and A. Coreau. 2009. Female polymorphisms, sexual conflict and limits to speciation processes in animals. Evol. Ecol. 23:93.

Swevers, L., and K. Iatrou. 2003. The ecdysone regulatory cascade and ovarian development in lepidopteran insects: insights from the silkmoth paradigm. Insect Biochem. Mol. Biol. 33:1285-1297.

Takahashi, Y., J. Yoshimura, S. Morita, and M. Watanabe. 2010. Negative frequency dependent selection in female color polymorphism of a damselfly. Evolution 64:3620-3628.

Takahashi, M., Y. Takahashi, and M. Kawata. 2018. Candidate genes associated with color morphs of female-limited polymorphisms of the damselfly *Ischnura senegalensis*. Heredity 122:81-92.

Takahashi, Y., and M. Watanabe. 2011. Male mate choice based on ontogenetic color changes of females in the damselfly *Ischnura senegalensis*. J. Ethol. 29:293-299.

Tanaka, K., O. Barmina, L. E. Sanders, M. N. Arbeitman, and A. Kopp. 2011. Evolution of sex-specific traits through changes in HOX-dependent doublesex expression. PLoS Biol. 9:e1001131.

bioRxiv preprint doi: https://doi.org/10.1101/714048; this version posted July 24, 2019. The copyright holder for this preprint (which was not certified by peer review) is the author/funder, who has granted bioRxiv a license to display the preprint in perpetuity. It is made available under aCC-BY-NC-ND 4.0 International license.

R Core Team. 2018. R: A language and environment for statistical computing. R Foundation for Statistical Computing. Vienna, Austria.

Thomas, J. A., J. W. H. Trueman, A. Rambaut, and J. J. Welch. 2013. Relaxed phylogenetics and the Palaeoptera problem: resolving deep ancestral splits in the insect phylogeny. Syst. Biol. 62:285-297.

Thomas, J. W., M. Cáceres, J. J. Lowman, C. B. Morehouse, M. E. Short, E. L. Baldwin, D. L. Maney, and C. L. Martin. 2008. The chromosomal polymorphism linked to variation in social behavior in the white-throated sparrow (*Zonotrichia albicollis*) is a complex rearrangement and suppressor of recombination. Genetics 179:1455-1468.

Thompson, M. J., and C. D. Jiggins. 2014. Supergenes and their role in evolution. Heredity 113:1-8.

Thurmond, J., J. L. Goodman, V. B. Strelets, H. Attrill, L. S. Gramates, S. J. Marygold, B. B. Matthews, G. Millburn, G. Antonazzo, V. Trovisco, and others. 201. FlyBase 2.0: the next generation. Nucleic Acids Res. 47:D759-D765.

Timmermans, M. J. T. N., S. W. Baxter, R. Clark, D. G. Heckel, H. Vogel, S. Collins, A. Papanicolaou, I. Fukova, M. Joron, M. J. Thompson, and others. 2014. Comparative genomics of the mimicry switch in *Papilio dardanus*. Proc. R Soc. Lond. B Biol. Sci. 281:20140465.

ten Tusscher, K. H. W. J., and P. Hogeweg. 2009. The role of genome and gene regulatory network canalization in the evolution of multi-trait polymorphisms and sympatric speciation. BMC Evol. Biol. 9:159.

UniProt Consortium. 2019. UniProt: a worldwide hub of protein knowledge. Nucleic Acids Res. 47:D506-D515.

Vera, J. C., C. W. Wheat, H. W. Fescemyer, M. J. Frilander, D. L. Crawford, I. Hanski, and J. H. Marden. 2008. Rapid transcriptome characterization for a nonmodel organism using 454 pyrosequencing. Mol. Ecol. 17:1636-1647.

Waller, J. T., and E. I. Svensson. 2017. Body size evolution in an old insect order: No evidence for Cope's Rule in spite of fitness benefits of large size. Evolution 71:2178-2193.

Wang, X. W., J. B. Luan, J. M. Li, Y. Y. Bao, C. X. Zhang, and S. S. Liu. 2010. *De novo* characterization of a whitefly transcriptome and analysis of its gene expression during development. BMC Genom. 11:400.

West-Eberhard, M. J. 2003. Developmental plasticity and evolution. Oxford University Press, New York, USA.

Wexler, J. R., D. C. Plachetzki, and A. Kopp. 2014. Pan-metazoan phylogeny of the DMRT gene family: a framework for functional studies. Dev. Genes Evol. 224:175-181.

Willink, B., and E. I. Svensson. 2017. Intra-and intersexual differences in parasite resistance and female fitness tolerance in a polymorphic insect. Proc. R Soc. Lond. B Biol. Sci. 284:20162407.

Willink, B., Duryea, M. C., & Svensson, E. I. 2019. Macroevolutionary origin and adaptive function of a polymorphic female signal involved in sexual conflict. Am. Nat. In press. doi:10.1086/705294

bioRxiv preprint doi: https://doi.org/10.1101/714048; this version posted July 24, 2019. The copyright holder for this preprint (which was not certified by peer review) is the author/funder, who has granted bioRxiv a license to display the preprint in perpetuity. It is made available under aCC-BY-NC-ND 4.0 International license.

Wood, A. R., M. A. Tuke, M. A. Nalls, D. G. Hernandez, S. Bandinelli, A. B. Singleton, D. Melzer, L. Ferrucci, T. M. Frayling, and M. N. Weedon. 2014. Another explanation for apparent epistasis. Nature 514:E3.

Wright, S. 1930. The genetical theory of natural selection: a review. J. Hered. 21:349-356.

Wright, S. 1931. Evolution in Mendelian populations. Genetics 16:97-159.

Xin, T., T. Xuan, J. Tan, M. Li, G. Zhao, and M. Li. 2013. The *Drosophila* putative histone acetyltransferase Enok maintains female germline stem cells through regulating Bruno and the niche. Dev. Biol. 384:1-12.

Yamasaki, Y., and Y. Nishida. 2006. Mi-2 chromatin remodeling factor functions in sensory organ development through proneural gene repression in *Drosophila*. Dev. Growth Differ. 48:411-418.

Yassin, A., E. K. Delaney, A. J. Reddiex, T. D. Seher, H. Bastide, N. C. Appleton, J. B. Lack, J. R. David, S. F. Chenoweth, J. E. Pool, and others. 2016. The pdm3 locus is a hotspot for recurrent evolution of female-limited color dimorphism in *Drosophila*. Curr. Biol. 26:2412-2422.

Zelditch, M. L., D. L. Swiderski, and H. D. Sheets. 2012. Geometric morphometrics for biologists: a primer. Academic Press, Cambridge, USA.

Zheng, W., T. Peng, W. He, and H. Zhang. 2012. High-throughput sequencing to reveal genes involved in reproduction and development in *Bactrocera dorsalis* (Diptera: Tephritidae). PLoS One 7:e36463.

Zhu, L., J. Wilken, N. B. Phillips, U. Narendra, G. Chan, S. M. Stratton, S. B. Kent, and M. A. Weiss. 2000. Sexual dimorphism in diverse metazoans is regulated by a novel class of intertwined zinc fingers. Genes Dev. 14:1750-1764.

Zinna, R., D. Emlen, L. C. Lavine, A. Johns, H. Gotoh, T. Niimi, and I. Dworkin. 2018. Sexual dimorphism and heightened conditional expression in a sexually selected weapon in the Asian rhinoceros beetle. Mol. Ecol. 27:5049-5072.

bioRxiv preprint doi: https://doi.org/10.1101/714048; this version posted July 24, 2019. The copyright holder for this preprint (which was not certified by peer review) is the author/funder, who has granted bioRxiv a license to display the preprint in perpetuity. It is made available under aCC-BY-NC-ND 4.0 International license.

Table 1. Number of differentially expressed (upregulated and downregulated) and similarly expressed (N.S.) genes, in comparisons between developmental phases and within female colour morphs of *I. elegans*. Developmental comparisons are performed between the *immature* and *transitional* phases (*early* colour development) and between the *transitional* and *mature* developmental phases (*late* colour development). A total of 27 females were sampled for this analysis, three of each colour morph in all three developmental phases.

Colour transition	Morph	Upregulated	Downregulated	N.S.
Early	A	197	5 200	20 983
	I	302	4 190	21 888
	O	978	4 685	20 717
Late	A	3 256	1 731	21 393
	I	364	355	25 661
	O	239	471	25 670

bioRxiv preprint doi: https://doi.org/10.1101/714048; this version posted July 24, 2019. The copyright holder for this preprint (which was not certified by peer review) is the author/funder, who has granted bioRxiv a license to display the preprint in perpetuity. It is made available under aCC-BY-NC-ND 4.0 International license.

Table 2. Ranking of the top ten most enriched GO terms for biological processes (Fisher's P < 0.01), in the subset of genes significantly downregulated during *early* colour development in all female morphs of *I. elegans*. The complete list of significantly enriched GO terms is presented in Table S4.

Rank	GO ID	Term	Annotated	Significant	Expected	Fisher's P
1	GO:0006412	translation	619	214	116.94	7.5e-18
2	GO:0015991	ATP hydrolysis coupled proton transport	44	21	8.31	1.3e-5
3	GO:0015986	ATP synthesis coupled proton transport	35	18	6.61	1.4e-5
4	GO:0006886	intracellular protein transport	237	71	44.77	2.0e-5
5	GO:1902600	proton transmembrane transport	115	55	21.73	6.5e-5
6	GO:0006511	ubiquitin-dependent protein catabolic process	119	38	22.48	4.3e-4
7	GO:0007264	small GTPase mediated signal transduction	215	60	40.62	7.1e-4
8	GO:0001731	formation of translation preinitiation complex	16	9	3.02	9.5e-4
9	GO:0006414	translational elongation	65	23	12.28	0.001
10	GO:0042423	catecholamine biosynthetic process	4	4	0.76	0.001

bioRxiv preprint doi: https://doi.org/10.1101/714048; this version posted July 24, 2019. The copyright holder for this preprint (which was not certified by peer review) is the author/funder, who has granted bioRxiv a license to display the preprint in perpetuity. It is made available under aCC-BY-NC-ND 4.0 International license.

Table 3. Ecdysone metabolism genes differentially regulated between A- and both I- and O-female morphs in *I. elegans*, during *late* colour development. Transcript sequences were blasted against annotated proteins in the *Drosophila melanogaster* (Dmel) genome. For each of the queried *I. elegans* sequences, we report the best Dmel hit, its corresponding gene name and inferred function.

Cluster ID	Best Dmel hit	Gene name	e-value	Function	References
19875.0	Cytochrome P450 307a1	*spo*	2.73e-9	Component or positive regulator of ecdysone biosynthesis in the ovary	Ono et al. (2006)
19875.1	Cytochrome P450 307a1	*spo*	4.64e-112	Component or positive regulator of ecdysone biosynthesis in the ovary	Ono et al. (2006)
24196.1	Ecdysone 20-monooxygenase / Cytochrome P450 314a1	*shd*	9.93e-103	Hydroxylates ecdysone to produce 20-hydroxyecdysone (20E)	Petryk et al. (2003)

bioRxiv preprint doi: https://doi.org/10.1101/714048; this version posted July 24, 2019. The copyright holder for this preprint (which was not certified by peer review) is the author/funder, who has granted bioRxiv a license to display the preprint in perpetuity. It is made available under aCC-BY-NC-ND 4.0 International license.

Table 4. Regulatory genes differentially expressed between A- and both I- and O-female morphs in *I. elegans*, during *late* colour development. Transcript sequences were blasted against annotated proteins in the *Drosophila melanogaster* (Dmel) genome. For each of the queried *I. elegans* sequences, we report the best Dmel hit, its corresponding gene name, e-value and inferred mode of regulation and function.

Cluster ID	Best Dmel hit	Gene name	e-value	Mode of regulation	Function	References
16360.1	Transcription termination factor, mitochondrial	*mTTF*	4.81e-32	Transcription factor	Regulates mitochondrial replication and transcription by interacting physically with helicase and polymerase enzymes	Roberti et al. (2005)
18749.0	T-related protein	*brachyenteron*	2.09e-49	Transcription factor	Fate determination of hindgut stem cells	Fox and Spradling (2009)
19883.1	Histone deacetylase complex subunit SAP30 homolog	*Sap30*	2.71e-58	Post-translational modification	Part of a correpressor complex that regulates G2/M cell cycle progression	Laherty et al. (1998)
28078.0	Ecdysone-induced protein E74	*Eip74EF*	1.01e-52	Transcription factor	Promotes germline proliferation and maintenance in ovaries	Ables and Drummond-Barbosa (2010)
31494.0	Enhancer of split mbeta protein	*E(spl)mbeta-HLH*	7.48e-20	Transcription factor	Repression of neural cell fate in response to Notch signalling	Jennings et al. (1994)
36913.0	Vrille	*vri*	7.43e-46	Transcription factor	Control of circadian rhythm, cardiac aging, ecdysone target in the ovary, associated with follicle cell maintenance and proliferation	Cyran et al. (2003); Monnier et al. (2012); Ables et al. (2016)
41360.2	Chromodomain-helicase-DNA-binding protein Mi-2 homolog	*Mi-2*	~ 0	Chromatin remodelling	Proneural gene repression	Yamasaki and Nishida (2006)
42782.0	Bunched	*bun*	6.00e-31	Transcription factor	Ovarian follicle cell development and migration, eggshell formation, neurblast proliferation, mushroom body development	Dobens et al. (1997); Dobens et al. (2000); Kim et al. (2009)
44536.0	Traffic jam	*tj*	2.66e-29	Transcription factor	Ovarian follicle cell migration, maintenance of ovarian stem cells	Gunawan et al. (2013); Panchal et al. (2017)
44568.1	Histone acetyltransferase	*enok*	8.66e-110	Post-translational modification	Neuroblast proliferation, maintenance of ovarian germ cells	Scott et al. (2001); Xin et al. (2013)
46100.0	Heterogeneous	*Hrb98DE*	2.93e-36	mRNA	maintenance and	He and

bioRxiv preprint doi: https://doi.org/10.1101/714048; this version posted July 24, 2019. The copyright holder for this preprint (which was not certified by peer review) is the author/funder, who has granted bioRxiv a license to display the preprint in perpetuity. It is made available under aCC-BY-NC-ND 4.0 International license.

	nuclear ribonucleoprotein A1			splicing and export	differentiation of ovarian germ cells,	Smith (2009); Ji and Tulin (2012)
46510.1	Homeotic protein Sex combs reduced	*Scr*	3.80e-46	Transcription factor	Induces and responds to the expression of *dsx* during sexual differentiation of somatic tissues	Barmina and Kopp (2007); Tanaka et al. (2011)
47599.1	Doublesex-Mab related 99B	*dmrt99B*	5.82e-20	Transcription factor	Integrates sex-determining, patterning and hormonal signals during somatic sexual differentiation	Kopp (2012)

bioRxiv preprint doi: https://doi.org/10.1101/714048; this version posted July 24, 2019. The copyright holder for this preprint (which was not certified by peer review) is the author/funder, who has granted bioRxiv a license to display the preprint in perpetuity. It is made available under aCC-BY-NC-ND 4.0 International license.

Figures

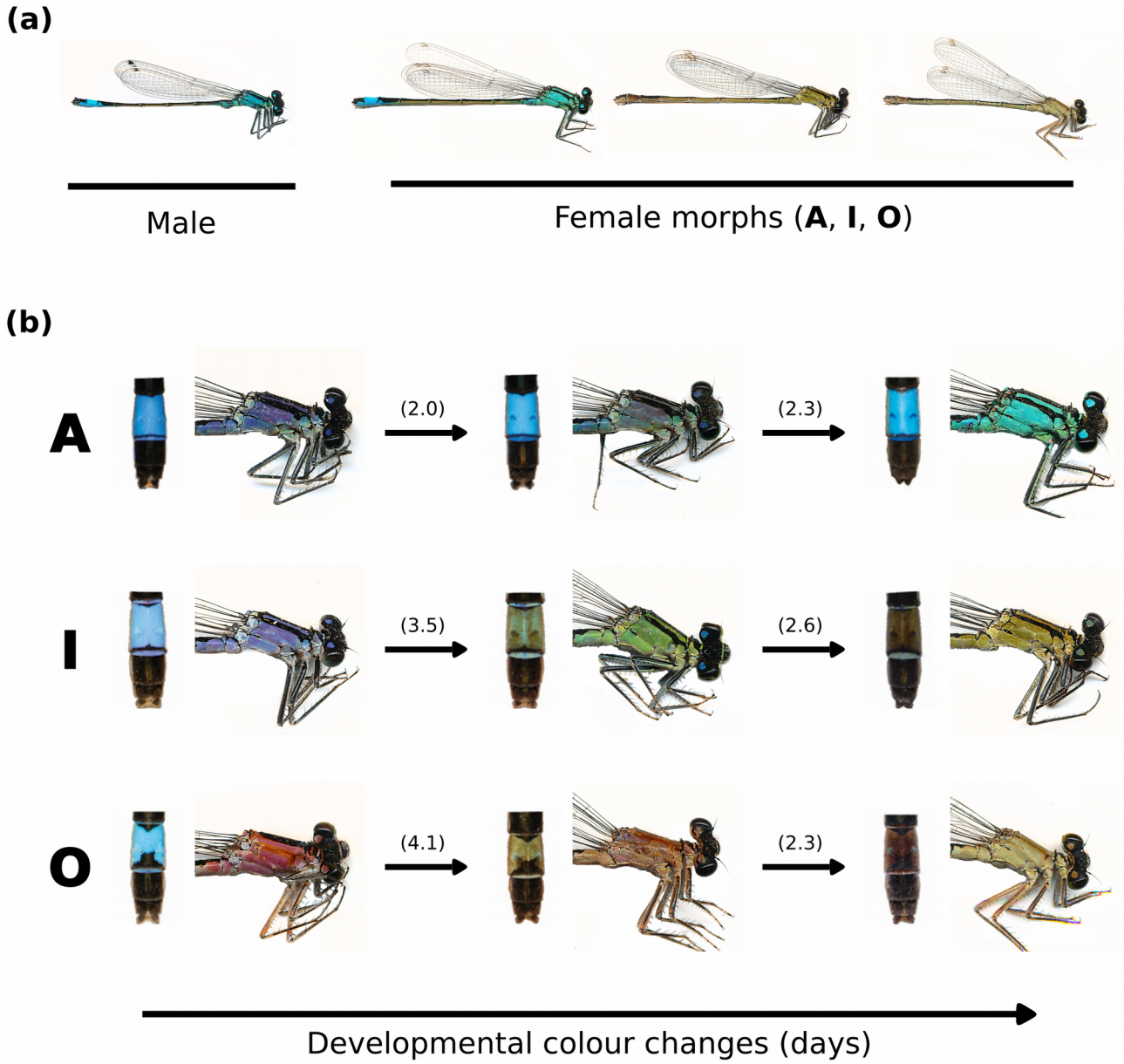

Figure 1. Heritable colour polymorphism and ontogenetic colour changes in females of the Common Bluetail damselfly (*Ischnura elegans*). **(a)** Male and the three female-limited colour morphs of *I. elegans* in their final, sexually mature developmental phase. The colour pattern of sexually mature A-females is remarkably similar to that of males, and hence they are considered to be male mimics. **(b)** Ontogenetic colour changes in the distal abdomen segments (left) and the thorax (right) of females of the three colour morphs in *I. elegans*. The columns correspond to females in the *immature*, *transitional* and *mature* developmental colour phases. The rows represent

bioRxiv preprint doi: https://doi.org/10.1101/714048; this version posted July 24, 2019. The copyright holder for this preprint (which was not certified by peer review) is the author/funder, who has granted bioRxiv a license to display the preprint in perpetuity. It is made available under aCC-BY-NC-ND 4.0 International license.

colour changes within each heritable morph. The numbers in parenthesis give the mean number of days for each colour transition, when females were kept in large outdoor mesocosm enclosures from their immature phase until sexual maturity (see Fig. S1). In A-females, the thorax colour changes during sexual development from violet to dull violet-turquoise, and finally to bright turquoise-blue. In I- and O-females, both thorax and distal abdomen undergo noticeable colour changes presumably involving extensive pigmentation. While the thoracic colour patterns of these two morphs are different, they share developmental darkening as the blue patch in the distal abdomen portion becomes completely concealed at sexual maturity. A- and I- females express very similar immature phases. However, these two morphs can be distinguished by the black “arrow-like” pattern in the eighth abdominal segment, which is thicker and marked by a central notch in I-females compared to A-females.

bioRxiv preprint doi: https://doi.org/10.1101/714048; this version posted July 24, 2019. The copyright holder for this preprint (which was not certified by peer review) is the author/funder, who has granted bioRxiv a license to display the preprint in perpetuity. It is made available under aCC-BY-NC-ND 4.0 International license.

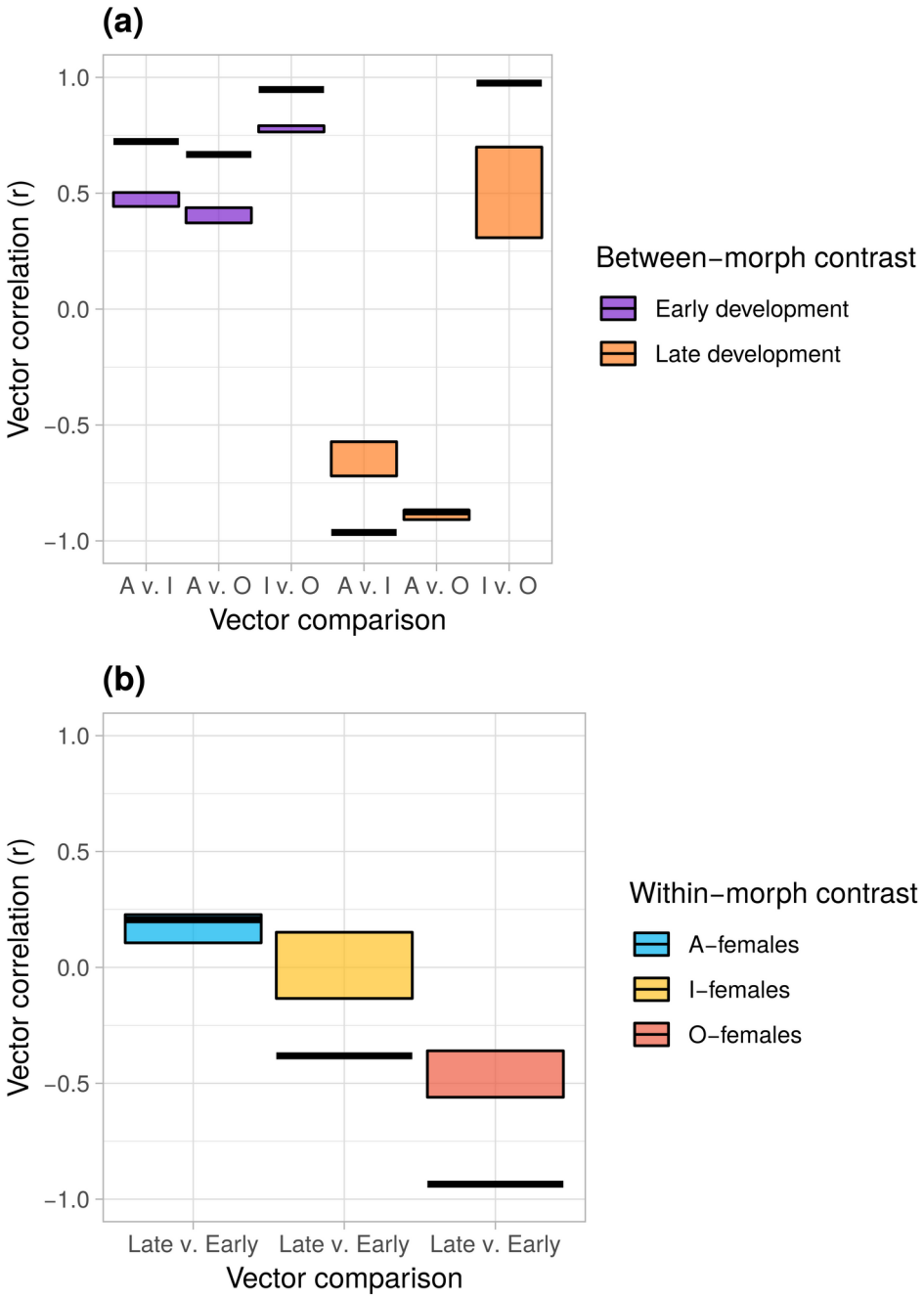

Figure 2. Vector correlations of gene expression contrasts. We tested for overall similarity in the expression changes underlying colour development **(a)** between all female-morph pairwise comparisons during *early* and *late* colour development, and **(b)** between *early* and *late* colour development within each female morph. Vector correlations (r) indicate the similarity in the direction of change in gene expression between two vectors of developmental contrasts. Values close to 1 suggest that the two vectors are nearly identical in direction, whereas values close to -1 suggest developmental regulation of gene expression is opposite in direction between the two vectors. The black horizontal lines show correlation values for experimental vectors (sets of

bioRxiv preprint doi: https://doi.org/10.1101/714048; this version posted July 24, 2019. The copyright holder for this preprint (which was not certified by peer review) is the author/funder, who has granted bioRxiv a license to display the preprint in perpetuity. It is made available under aCC-BY-NC-ND 4.0 International license.

differentially expressed genes, see Methods), the coloured boxes show the 95 percentile of empirical distributions of 10 000 contrast vectors of the same length as the experimental vectors, but including a random sample of all genes whether DE or not.

bioRxiv preprint doi: https://doi.org/10.1101/714048; this version posted July 24, 2019. The copyright holder for this preprint (which was not certified by peer review) is the author/funder, who has granted bioRxiv a license to display the preprint in perpetuity. It is made available under aCC-BY-NC-ND 4.0 International license.

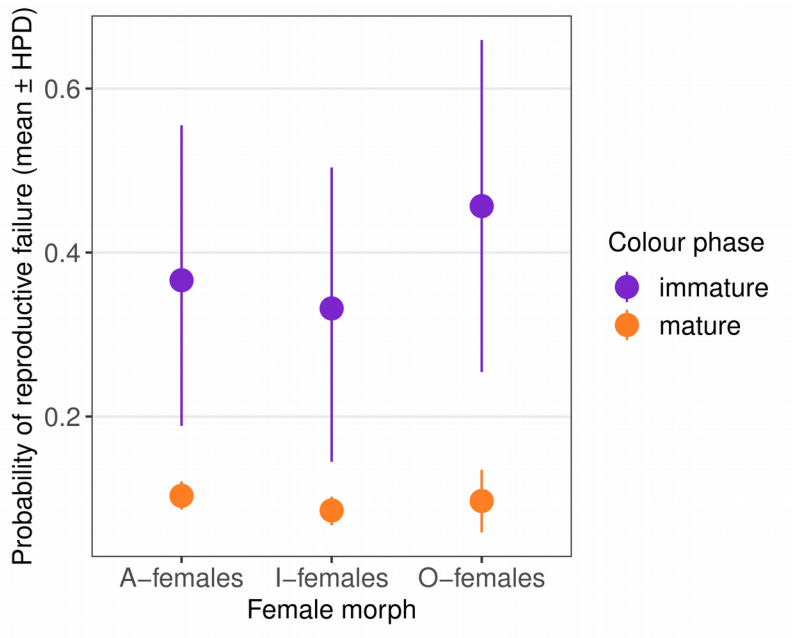

Figure 3. Probability of reproductive failure, quantified as the proportion of mated females laying no viable eggs, among three female morphs and two developmental colour phases of *I. elegans*. The symbols show the posterior mean and 95% highest posterior density (HPD) intervals of parameter estimates in a binomial mixed-effect model fitted by MCMC.

bioRxiv preprint doi: https://doi.org/10.1101/714048; this version posted July 24, 2019. The copyright holder for this preprint (which was not certified by peer review) is the author/funder, who has granted bioRxiv a license to display the preprint in perpetuity. It is made available under aCC-BY-NC-ND 4.0 International license.

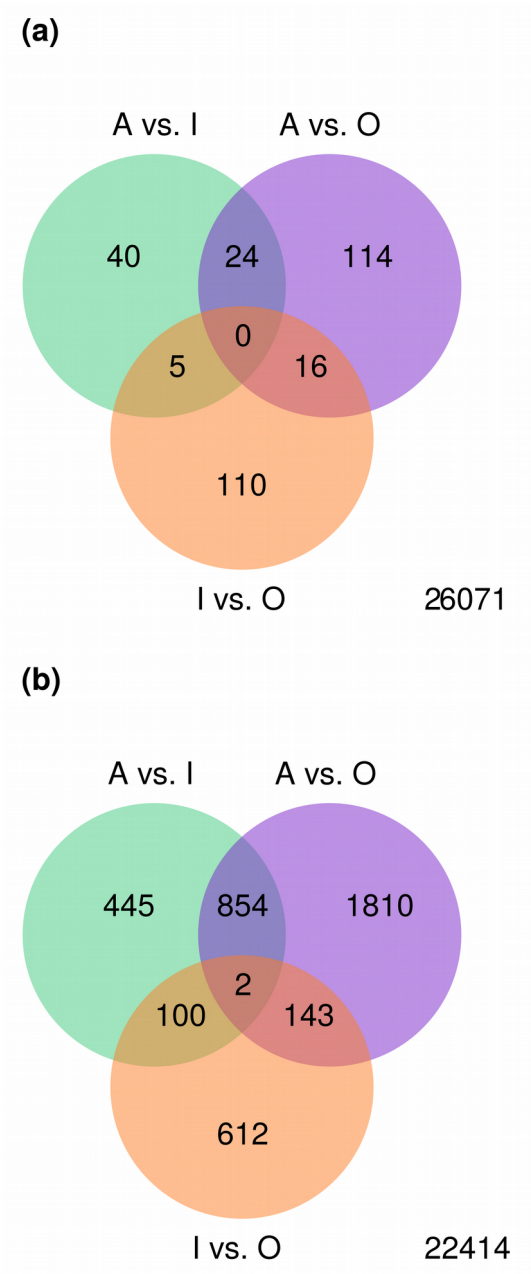

Figure 4. Venn diagram showing the genes that were differentially regulated across colour development, between pairs of female morphs of *I. elegans* (i.e. genes with significant differences between morphs in the direction or magnitude of developmental changes; contrast group (3); Table S2). **(a)** *early* colour development, **(b)** *late* colour development. The number of genes with no evidence of morph differences in differential expression between developmental colour phases is shown in the bottom right corner of each plot.

bioRxiv preprint doi: https://doi.org/10.1101/714048; this version posted July 24, 2019. The copyright holder for this preprint (which was not certified by peer review) is the author/funder, who has granted bioRxiv a license to display the preprint in perpetuity. It is made available under aCC-BY-NC-ND 4.0 International license.

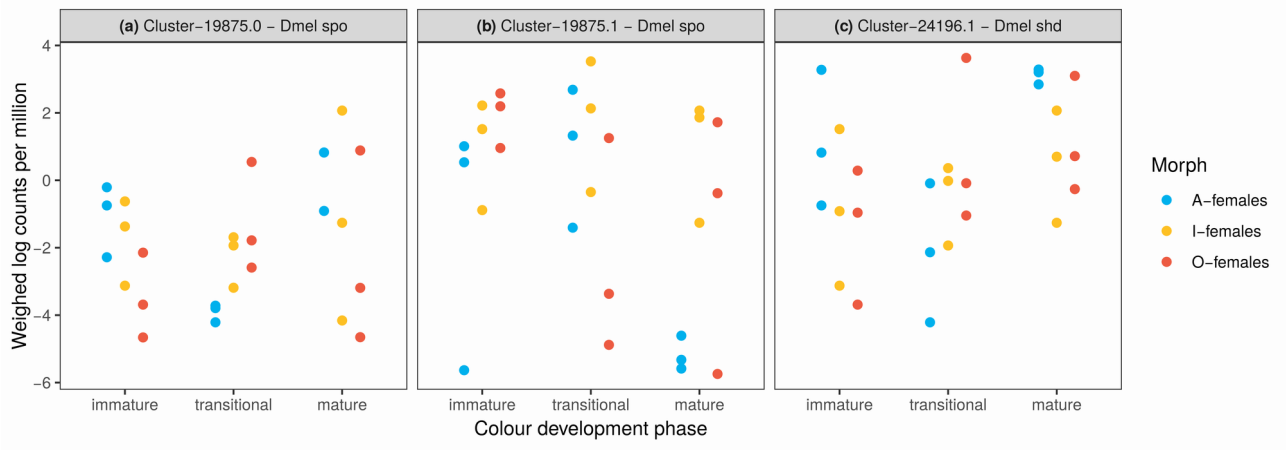

Figure 5. Expression patterns of ecdysone metabolism genes differentially regulated between A- and both I- and O-females during *late* colour development of *I. elegans*. Expression data (log counts per million) have been weighed by within-sample variability and by the mean-variance relationship among genes, using 'voom' (see Methods). Corresponding gene products and inferred functions in *D. melanogaster* (Dmel) are shown in Table 3.

bioRxiv preprint doi: https://doi.org/10.1101/714048; this version posted July 24, 2019. The copyright holder for this preprint (which was not certified by peer review) is the author/funder, who has granted bioRxiv a license to display the preprint in perpetuity. It is made available under aCC-BY-NC-ND 4.0 International license.

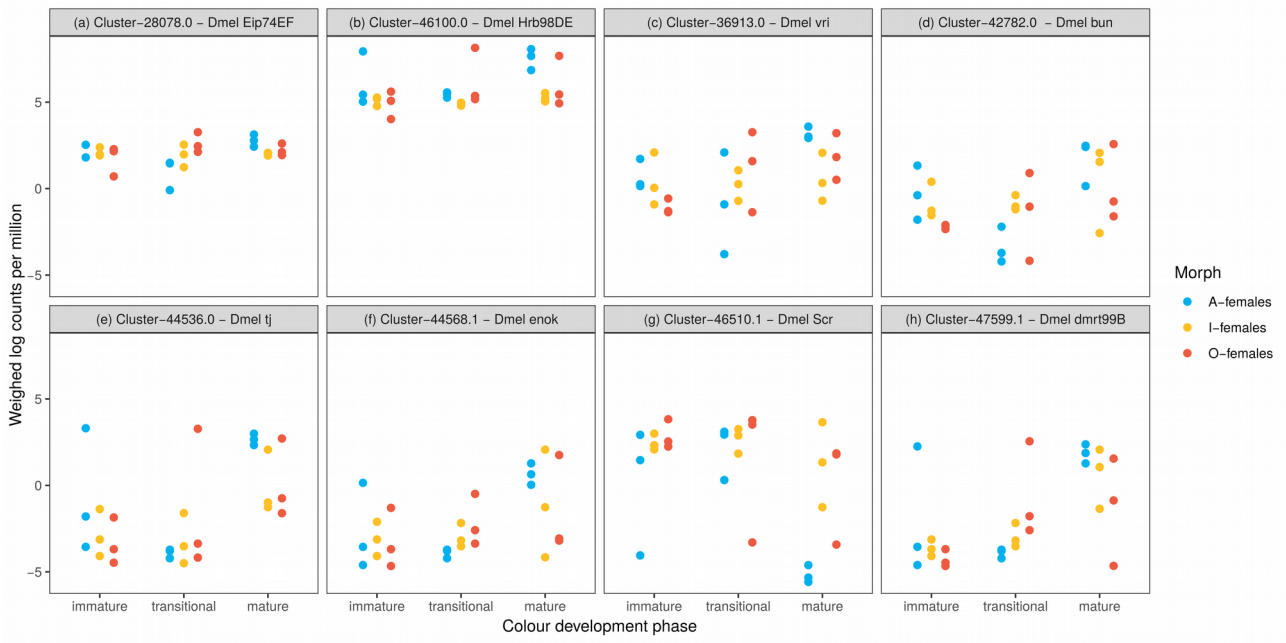

Figure 6. Regulatory genes differentially regulated between A- and both I- and O-females, during *late* colour development of *I. elegans*. The circles indicate expression levels of genes with inferred roles in regulating reproductive development (**a**-**f**) and sexual differentiation (**g**-**h**) in *D. melanogaster*. Expression data (log counts per million) have been weighed by within-sample variability and by the mean-variance relationship among genes, using 'voom' (see Methods). Corresponding gene products and inferred modes of regulation and functions are shown in Table 4.

bioRxiv preprint doi: https://doi.org/10.1101/714048; this version posted July 24, 2019. The copyright holder for this preprint (which was not certified by peer review) is the author/funder, who has granted bioRxiv a license to display the preprint in perpetuity. It is made available under aCC-BY-NC-ND 4.0 International license.

Supporting Material

Gene expression changes during female reproductive development in a colour polymorphic insect

B. Willink, M. C. Duryea, C. Wheat and E. I. Svensson

Figure S1. Duration of colour development in the three female morphs of *Ischnura elegans*. A total of 212 emerged females (N_A = 66 , N_I = 108, N_O = 38) were raised in outdoor enclosures and the first day of observation of each developmental colour phase was recorded for surviving individuals. The points show the number of days to reach the *transitional* colour phase (end of *early* colour development) and the *mature* colour phase (end of *late* colour development), for females raised on three consecutive years. A mixed effect model fitted by MCMC, with time-to-colour-phase as the response variable and the interaction between morph (A- I- or O-females), colour development (*early* or *late*) and year (2015, 2016 or 2017) as predictor variables, uncovered a significantly shorter duration of *early* colour development of A-females compared to I- and O-females in 2015 ($PMCM_{A\ vs\ I} < 0.001$, $PMCMC_{A\ vs\ O} < 0.001$) and 2016 ($PMCM_{A\ vs\ I} = 0.005$, $PMCMC_{A\ vs\ O} = 0.008$). The statistical model assumed a Poisson error distribution and a random effect of the enclosure position on the fixed effect variance.

bioRxiv preprint doi: https://doi.org/10.1101/714048; this version posted July 24, 2019. The copyright holder for this preprint (which was not certified by peer review) is the author/funder, who has granted bioRxiv a license to display the preprint in perpetuity. It is made available under aCC-BY-NC-ND 4.0 International license.

Table S1. Individuals sampled for the *de novo* transcriptome assembly of *I. elegans* used in this study. All individuals come from local populations in Southern Sweden and they were collected either in the field, at their populations of origin, or in experimental outdoor enclosures (Mesocosms), in a field station in the same area. Samples were collected during the mating seasons of 2012 and 2015. The first 27 samples were used for the differential expression analysis in this study.

ID	Sex	Morph	Colour phase	Season	Collection site	Mating status
T214	Female	A	immature	2015	Field	Unmated
T43	Female	A	immature	2015	Field	Unmated
T44	Female	A	immature	2015	Field	Unmated
T126	Female	A	transitional	2015	Field	Unmated
T127	Female	A	transitional	2015	Field	Unmated
T45	Female	A	transitional	2015	Field	Unmated
T128	Female	A	mature	2015	Field	Unmated
T129	Female	A	mature	2015	Field	Unmated
T130	Female	A	mature	2015	Field	Unmated
T213	Female	I	immature	2015	Field	Unmated
T41	Female	I	immature	2015	Field	Unmated
T42	Female	I	immature	2015	Field	Unmated
249	Female	I	transitional	2015	Field	Unmated
256	Female	I	transitional	2015	Field	Unmated
266	Female	I	transitional	2015	Field	Unmated
T11	Female	I	mature	2015	Field	Mated
T29	Female	I	mature	2015	Field	Mated
T35	Female	I	mature	2015	Field	Mated
T165	Female	O	immature	2015	Field	Unmated
T54	Female	O	immature	2015	Field	Unmated
T63	Female	O	immature	2015	Field	Unmated
T21	Female	O	transitional	2015	Field	Mated
T217	Female	O	transitional	2015	Field	Unmated
T97	Female	O	transitional	2015	Field	Unmated
T96	Female	O	mature	2015	Field	Unmated
188	Female	O	mature	2015	Field	Unmated
248	Female	O	mature	2015	Field	Unmated
T234	Female	I	mature	2015	Mesocosm	Unmated
T274B7	Female	I	mature	2015	Mesocosm	Mated
T267B5-6	Female	I	mature	2015	Mesocosm	Mated
T238	Female	I	mature	2015	Mesocosm	Mated
T278B7	Female	I	mature	2015	Mesocosm	Mated
T242	Female	I	mature	2015	Mesocosm	Mated
T250	Female	I	mature	2015	Mesocosm	Unmated
T284B7	Female	I	mature	2015	Mesocosm	Unmated
T251	Female	I	mature	2015	Mesocosm	Unmated

bioRxiv preprint doi: https://doi.org/10.1101/714048; this version posted July 24, 2019. The copyright holder for this preprint (which was not certified by peer review) is the author/funder, who has granted bioRxiv a license to display the preprint in perpetuity. It is made available under aCC-BY-NC-ND 4.0 International license.

ID	Sex	Morph	Colour phase	Season	Collection site	Mating status
T224	Female	I	mature	2015	Mesocosm	Mated
T280B7	Female	I	mature	2015	Mesocosm	Mated
T220	Female	I	mature	2015	Mesocosm	Mated
T235	Female	A	mature	2015	Mesocosm	Unmated
T273B5-6	Female	A	mature	2015	Mesocosm	Unmated
T244	Female	A	mature	2015	Mesocosm	Unmated
T236	Female	A	mature	2015	Mesocosm	Mated
T274B5-6	Female	A	mature	2015	Mesocosm	Mated
T273B7	Female	A	mature	2015	Mesocosm	Mated
T230	Female	A	mature	2015	Mesocosm	Unmated
T280B5-6	Female	A	mature	2015	Mesocosm	Unmated
T253	Female	A	mature	2015	Mesocosm	Unmated
T222	Female	A	mature	2015	Mesocosm	Mated
T284B5-6	Female	A	mature	2015	Mesocosm	Mated
T288B7	Female	A	mature	2015	Mesocosm	Mated
T172	Female	I	mature	2015	Mesocosm	Unmated
T189	Female	I	mature	2015	Mesocosm	Unmated
T195	Female	I	mature	2015	Mesocosm	Unmated
T171	Female	A	mature	2015	Mesocosm	Unmated
T188	Female	A	mature	2015	Mesocosm	Unmated
T194	Female	A	mature	2015	Mesocosm	Unmated
T70	Female	A	mature	2015	Mesocosm	Mated
T81	Female	A	mature	2015	Mesocosm	Mated
50	Female	A	mature	2012	Mesocosm	Unknown
54	Female	A	mature	2012	Mesocosm	Unknown
70	Female	A	mature	2012	Mesocosm	Unknown
80	Female	A	mature	2012	Mesocosm	Unknown
49	Female	I	mature	2012	Mesocosm	Unknown
51	Female	I	mature	2012	Mesocosm	Unknown
52	Female	I	mature	2012	Mesocosm	Unknown
53	Female	I	mature	2012	Mesocosm	Unknown
55	Female	I	mature	2012	Mesocosm	Unknown
56	Female	I	mature	2012	Mesocosm	Unknown
31	Female	A	mature	2012	Mesocosm	Unknown
42	Female	A	mature	2012	Mesocosm	Unknown
43	Female	A	mature	2012	Mesocosm	Unknown
47	Female	A	mature	2012	Mesocosm	Unknown
33	Female	I	mature	2012	Mesocosm	Unknown
35	Female	I	mature	2012	Mesocosm	Unknown
44	Female	I	mature	2012	Mesocosm	Unknown
46	Female	I	mature	2012	Mesocosm	Unknown

bioRxiv preprint doi: https://doi.org/10.1101/714048; this version posted July 24, 2019. The copyright holder for this preprint (which was not certified by peer review) is the author/funder, who has granted bioRxiv a license to display the preprint in perpetuity. It is made available under aCC-BY-NC-ND 4.0 International license.

ID	Sex	Morph	Colour phase	Season	Collection site	Mating status
8	Female	A	mature	2012	Mesocosm	Unknown
36	Female	A	mature	2012	Mesocosm	Unknown
39	Female	A	mature	2012	Mesocosm	Unknown
40	Female	A	mature	2012	Mesocosm	Unknown
15	Female	I	mature	2012	Mesocosm	Unknown
26	Female	I	mature	2012	Mesocosm	Unknown
38	Female	I	mature	2012	Mesocosm	Unknown
57	Female	I	mature	2012	Mesocosm	Unknown

Table S2. Contrast matrices for the three types of comparisons of differential gene expression in females of *Ischnura elegans*, given the interaction term in the model formula: ~0 + Morph + Colour Phase + Morph: Colour Phase. There are three morphs (Androchrome, Infuscans, and Obsoleta) and three colour development phases: *immature* (Imm), *transitional* (Tra) and *mature* (Mat). The *immature* colour phase is treated as the intercept within each morph (i.e. 'Androchrome' refers to *immature* Androchrome females). Three types of contrasts were estimated: (1) contrasts among morphs within each colour phase, (2) contrasts between subsequent colour phases within morphs and (3) and contrasts between developmental changes among morphs. For (3), developmental changes corresponded to one of two developmental windows: *early* colour development (E), between the *immature* and *transitional* phase and *late* colour development (L), between the *transitional* and *mature* colour phase.

(1) Among morphs	**Contrasts**								
Levels	AImmvsIImm	AImmvsOImm	IImmvsOImm	ATravsITra	ATravsOTra	ITravsOTra	AMatvsIMat	AMatvsOMat	IMatvsOMat
Androchrome	1	1	0	0	0	0	0	0	0
Infuscans	-1	0	1	0	0	0	0	0	0
Obsoleta	0	-1	-1	0	0	0	0	0	0
AgeTransitional	0	0	0	1	1	0	0	0	0
Infuscans.AgeTransitional	0	0	0	-1	0	1	0	0	0
Obsoleta.AgeTransitional	0	0	0	0	-1	-1	0	0	0
AgeMature	0	0	0	0	0	0	1	1	0
Infuscans.AgeMature	0	0	0	0	0	0	-1	0	1
Obsoleta.AgeMature	0	0	0	0	0	0	0	-1	-1

(2) Between phases	**Contrasts**					
Levels	ATravsAImm	ITravsIImm	OTravsOImm	AMatvsATra	IMatvsITra	OMatvsOTra
Androchrome	-1	0	0	0	0	0
Infuscans	0	-1	0	0	0	0
Obsoleta	0	0	-1	0	0	0
AgeTransitional	1	0	0	-1	0	0
Infuscans.AgeTransitional	0	1	0	0	-1	0
Obsoleta.AgeTransitional	0	0	1	0	0	-1

AgeMature	0	0	0	1	0	0
Infuscans.AgeMature	0	0	0	0	1	0
Obsoleta.AgeMature	0	0	0	0	0	1

(3) Phase differences among morphs **Contrasts**

Levels	AEvsIE	AEvsOE	IEvsOE	ALvsIL	ALvsOL	ILvsOL
Androchrome	-1	-1	0	0	0	0
Infuscans	1	0	-1	0	0	0
Obsoleta	0	1	1	0	0	0
AgeTransitional	1	1	0	-1	-1	0
Infuscans.AgeTransitional	-1	0	1	1	0	-1
Obsoleta.AgeTransitional	0	-1	-1	0	1	1
AgeMature	0	0	0	1	1	0
Infuscans.AgeMature	0	0	0	-1	0	1
Obsoleta.AgeMature	0	0	0	0	-1	-1

bioRxiv preprint doi: https://doi.org/10.1101/714048; this version posted July 24, 2019. The copyright holder for this preprint (which was not certified by peer review) is the author/funder, who has granted bioRxiv a license to display the preprint in perpetuity. It is made available under aCC-BY-NC-ND 4.0 International license.

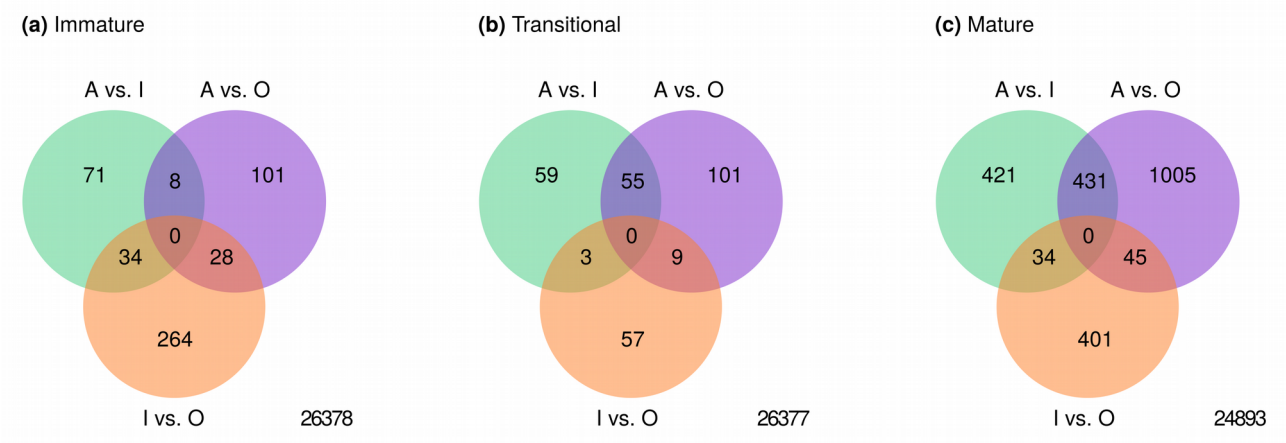

Figure S2. Venn diagram of differentially expressed genes between morphs and within developmental colour phase in females of *I. elegans* (contrast group (1); Table S2). Three females of each morph were sampled at each of three stages of adult colour development **(a)** *immature*, **(b)** *transitional* and **(c)** *mature*. The number of genes with no evidence of morph differences in differential expression between developmental colour phases is shown in the bottom right corner of each plot.

bioRxiv preprint doi: https://doi.org/10.1101/714048; this version posted July 24, 2019. The copyright holder for this preprint (which was not certified by peer review) is the author/funder, who has granted bioRxiv a license to display the preprint in perpetuity. It is made available under aCC-BY-NC-ND 4.0 International license.

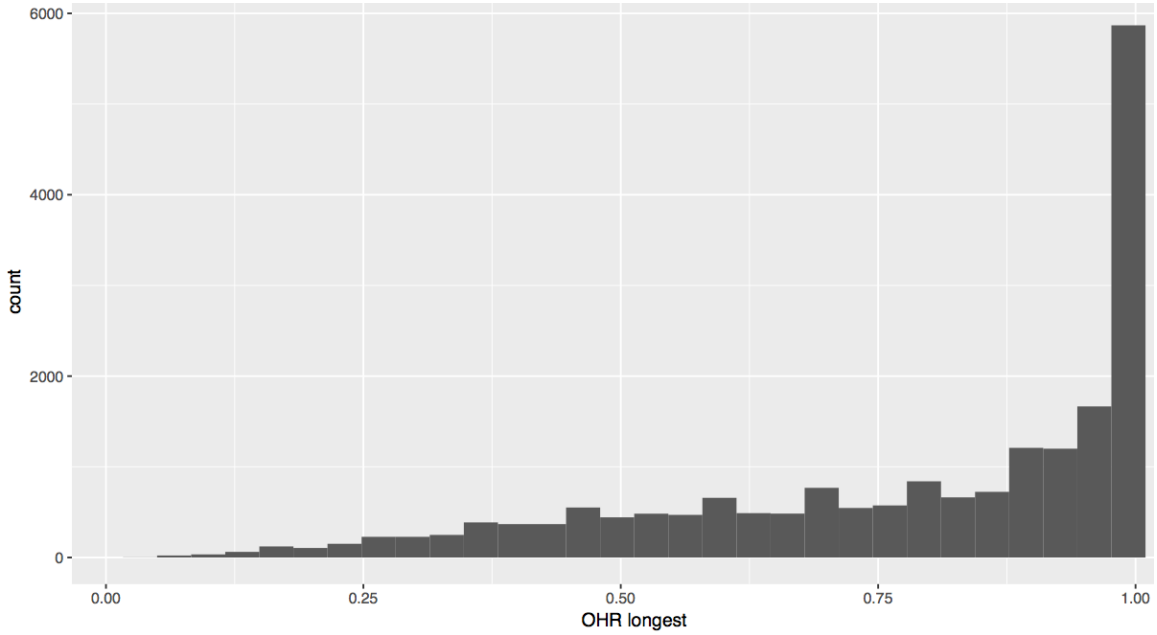

Figure S3. Histogram of ortholog hit ratios (OHR) for *Ischnura elegans* transcripts with orthologs in the *Calopteryx splendens* genome. The OHR represents the fraction of the protein coding sequences in the *C. splendess* genome that is covered by a single (longest) *I. elegans* transcript. Around 70% of the sequences are covered to 70% or more of their full expected length, indicating the transcriptome quality is acceptable.

bioRxiv preprint doi: https://doi.org/10.1101/714048; this version posted July 24, 2019. The copyright holder for this preprint (which was not certified by peer review) is the author/funder, who has granted bioRxiv a license to display the preprint in perpetuity. It is made available under aCC-BY-NC-ND 4.0 International license.

Table S3. Distribution of protein clusters in the *Calopteryx splendens* genome with orthologs in the *Ischnura elegans* transctriptome. The first column indicates the sequence length in the *C. splendens* genome and the remaining columns show the ortholog hit ratio (OHR) of the longest transcript in the *I. elegans* transcriptome mapped to each *C. splendens* protein coding sequence. The OHR represents the fraction of the protein coding sequence that is covered by a single (longest) *I. elegans* transcript. Around 70% of the sequences are covered to 70% or more of their full expected length, indicating the transcriptome quality is acceptable.

	Assembly length quantile									
Length	**0-0.1**	**0.11-0.2**	**0.21-0.3**	**0.31-0.4**	**0.41-0.5**	**0.51-0.6**	**0.61-0.7**	**0.71-0.8**	**0.81-0.9**	**0.9-1.0**
0-100	0	0	6	44	116	155	201	265	320	1033
101-200	0	21	119	233	337	410	484	629	866	3213
201-500	13	127	176	226	261	322	412	564	940	4858
501-1000	12	30	21	29	38	56	105	481	374	1938
1001-2000	2	7	3	9	8	8	15	46	117	491
2001-5000	0	0	0	3	1	1	03	5	15	85
5001-10000	0	0	0	0	0	1	0	0	2	6
>10000	0	0	0	0	0	0	0	0	0	0
Sum	27	185	325	544	761	953	1220	1689	2634	11624

bioRxiv preprint doi: https://doi.org/10.1101/714048; this version posted July 24, 2019. The copyright holder for this preprint (which was not certified by peer review) is the author/funder, who has granted bioRxiv a license to display the preprint in perpetuity. It is made available under aCC-BY-NC-ND 4.0 International license.

Table S4. GO terms for significantly enriched biological processes (Fisher's P < 0.01) in the subset of downregulated genes shared by all female morphs of of *I. elegans*, during *early* colour development.

Rank	GO ID	Term	Annotated	Significant	Expected	Fisher's P
1	GO:0006412	translation	619	214	116.94	7.5e-18
2	GO:0015991	ATP hydrolysis coupled proton transport	44	21	8.31	1.3e-5
3	GO:0015986	ATP synthesis coupled proton transport	35	18	6.61	1.4e-5
4	GO:0006886	intracellular protein transport	237	71	44.77	2.0e-5
5	GO:1902600	proton transmembrane transport	115	55	21.73	6.5e-5
6	GO:0006511	ubiquitin-dependent protein catabolic process	119	38	22.48	4.3e-4
7	GO:0007264	small GTPase mediated signal transduction	215	60	40.62	7.1e-4
8	GO:0001731	formation of translation preinitiation complex	16	9	3.02	9.5e-4
9	GO:0006414	translational elongation	65	23	12.28	0.001
10	GO:0042423	catecholamine biosynthetic process	4	4	0.76	0.001
11	GO:0016579	protein deubiquitination	47	18	8.88	0.001
12	GO:0009108	coenzyme biosynthetic process	120	36	22.67	0.002
13	GO:0048193	Golgi vesicle transport	43	16	8.12	0.004
14	GO:0045116	protein neddylation	5	4	0.94	0.005
15	GO:0006465	signal peptide processing	5	4	0.94	0.005
16	GO:0042773	ATP synthesis coupled electron transport	23	10	4.35	0.006
17	GO:0051603	proteolysis involved in cellular protein catabolic process	139	47	26.26	0.006
18	GO:0006413	translational initiation	140	44	26.45	0.007
19	GO:0019243	methylglyoxal catabolic process to D-lactate via S-lactoyl-glutathione	3	3	0.57	0.007
20	GO:0006826	iron ion transport	14	7	2.64	0.008
21	GO:0035194	posttranscriptional gene silencing by RNA	11	6	2.08	0.009
22	GO:0006163	purine nucleotide metabolic process	208	68	39.3	0.010

1145

bioRxiv preprint doi: https://doi.org/10.1101/714048; this version posted July 24, 2019. The copyright holder for this preprint (which was not certified by peer review) is the author/funder, who has granted bioRxiv a license to display the preprint in perpetuity. It is made available under aCC-BY-NC-ND 4.0 International license.

Table S5. GO terms for significantly enriched biological processes (Fisher's P < 0.01) in the subset of upregulated genes for each female morph of of *I. elegans*, during *early* colour development. GO terms with fewer than 3 annotated genes are excluded.

Rank	GO ID	Term	Annotated	Significant	Expected	Fisher's P
A-females						
1	GO:0090304	nucleic acid metabolic process	1832	16	7.77	0.002
I-females						
1	GO:0006278	RNA-dependent DNA biosynthetic process	206	7	1.08	8.4e-5
2	GO:1901136	carbohydrate derivative catabolic process	60	3	0.31	0.004
O-females						
1	GO:0071555	cell wall organization	21	5	0.55	1.7e-4
2	GO:0005980	glycogen catabolic process	5	3	0.13	1.7e-4
3	GO:0072488	ammonium transmembrane transport	6	3	0.16	3.3-4
4	GO:0006355	regulation of transcription, DNA-templated	593	29	15.54	7.6e-4
5	GO:0007094	mitotic spindle assembly checkpoint	9	3	0.24	0.001
6	GO:0055123	digestive system development	5	2	0.13	0.006
7	GO:0045165	cell fate commitment	6	2	0.16	0.010

1150

bioRxiv preprint doi: https://doi.org/10.1101/714048; this version posted July 24, 2019. The copyright holder for this preprint (which was not certified by peer review) is the author/funder, who has granted bioRxiv a license to display the preprint in perpetuity. It is made available under aCC-BY-NC-ND 4.0 International license.

Table S6. GO terms for significantly enriched biological processes (Fisher's P < 0.01) in the subset of downregulated genes for each female morph of of *I. elegans*, during *late* colour development. GO terms with fewer than 3 annotated genes are excluded.

Rank	GO ID	Term	Annotated	Significant	Expected	Fisher's P
A-females						
1	GO:0015986	ATP synthesis coupled proton transport	35	21	1.92	2.4e-18
2	GO:0055114	oxidation-reduction process	836	129	45.9	5.6e-17
3	GO:1902600	proton transmembrane transport	115	45	6.31	1.8e-16
4	GO:0022900	electron transport chain	36	26	1.98	1.4e-7
5	GO:0006120	mitochondrial electron transport, NADH to ubiquinone	7	6	0.38	1.8e-7
6	GO:0042773	ATP synthesis coupled electron transport	23	16	1.26	1.7e-6
7	GO:0006099	tricarboxylic acid cycle	30	9	1.65	2.1e-5
8	GO:0006108	malate metabolic process	11	5	0.6	1.7e-4
9	GO:0042775	mitochondrial ATP synthesis coupled electron transport	14	10	0.77	2.6e-4
10	GO:0006744	ubiquinone biosynthetic process	8	4	0.44	5.3e-4
11	GO:0034220	ion transmembrane transport	347	73	19.05	6.6e-4
12	GO:0070588	calcium ion transmembrane transport	22	6	1.21	9.3e-4
13	GO:0006777	Mo-molybdopterin cofactor biosynthetic process	10	4	0.55	0.001
14	GO:0019646	aerobic electron transport chain	5	3	0.27	0.002
15	GO:0016180	snRNA processing	11	4	0.6	0.002
16	GO:0015991	ATP hydrolysis coupled proton transport	44	8	2.42	0.002
17	GO:0022904	respiratory electron transport chain	29	20	1.59	0.008
I-females						
1	GO:0006633	fatty acid biosynthetic process	55	8	0.87	2.1e-6
2	GO:0006869	lipid transport	75	9	1.19	2.5e-6
3	GO:0035194	posttranscriptional gene silencing by RNA	11	3	0.17	5.8e-4
4	GO:0032259	methylation	224	10	3.55	0.003
5	GO:0006629	lipid metabolic process	281	17	4.45	0.007
6	GO:0006026	aminoglycan catabolic process	48	4	0.76	0.007
O-females						
1	GO:0035335	peptidyl-tyrosine dephosphorylation	46	5	0.75	8.4e-4
2	GO:0009157	deoxyribonucleoside monophosphate biosynthetic process	4	2	0.06	0.002
3	GO:0007062	sister chromatid cohesion	18	3	0.29	0.003
4	GO:0044772	mitotic cell cycle phase transition	38	4	0.62	0.003
5	GO:0009451	RNA modification	81	5	1.31	0.010

bioRxiv preprint doi: https://doi.org/10.1101/714048; this version posted July 24, 2019. The copyright holder for this preprint (which was not certified by peer review) is the author/funder, who has granted bioRxiv a license to display the preprint in perpetuity. It is made available under aCC-BY-NC-ND 4.0 International license.

1155 **Table S7.** GO terms for significantly enriched biological processes (Fisher's P < 0.01) in the subset of upregulated genes for each female morph of of *I. elegans*, during *late* colour development. GO terms with fewer than 3 annotated genes are excluded.

Rank	GO ID	Term	Annotated	Significant	Expected	Fisher's P
A-females						
1	GO:0006260	DNA replication	98	40	15.07	1.5e-5
2	GO:0034587	piRNA metabolic process	5	5	0.77	8.5e-5
3	GO:0071139	resolution of recombination intermediates	5	5	0.77	8.5e-5
4	GO:0006468	protein phosphorylation	452	99	69.49	9.5e-5
5	GO:0006281	DNA repair	167	49	25.67	1.3e-4
6	GO:0006261	DNA-dependent DNA replication	36	15	5.53	1.3e-4
7	GO:0000724	double-strand break repair via homologous recombination	15	8	2.31	7.1e-4
8	GO:0007049	cell cycle	190	64	29.21	8.2e-4
9	GO:0051304	chromosome separation	16	8	2.46	0.001
10	GO:0007076	mitotic chromosome condensation	7	5	1.08	0.001
11	GO:0090501	RNA phosphodiester bond hydrolysis	49	16	7.53	0.002
12	GO:0051276	chromosome organization	227	66	34.9	0.002
13	GO:0034314	Arp2/3 complex-mediated actin nucleation	17	8	2.61	0.002
14	GO:0007062	sister chromatid cohesion	18	8	2.77	0.003
15	GO:0007346	regulation of mitotic cell cycle	48	15	7.38	0.004
16	GO:0051301	cell division	62	18	9.53	0.004
17	GO:0097659	nucleic acid-templated transcription	718	142	110.38	0.006
18	GO:0000075	cell cycle checkpoint	36	12	5.53	0.006
19	GO:0016570	histone modification	78	21	11.99	0.006
20	GO:0006869	lipid transport	75	20	11.53	0.008
21	GO:0006355	regulation of transcription, DNA-templated	593	112	91.16	0.009
22	GO:0007017	microtubule-based process	159	36	24.44	0.009
23	GO:0051321	meiotic cell cycle	17	7	2.61	0.009
I-females						
1	GO:1902600	proton transmembrane transport	115	10	1.05	7.3e-8
2	GO:0006119	oxidative phosphorylation	38	5	0.35	2.2e-5
3	GO:0015893	drug transport	14	3	0.13	2.5e-4
4	GO:0019646	aerobic electron transport chain	5	2	0.05	8.0e-4
5	GO:0035725	sodium ion transmembrane transport	22	3	0.2	9.9e-4
6	GO:0045333	cellular respiration	72	8	0.66	0.002
7	GO:0022900	electron transport chain	36	5	0.33	0.003
8	GO:0006885	regulation of pH	11	2	0.1	0.004
9	GO:0009060	aerobic respiration	45	5	0.41	0.005
10	GO:0006754	ATP biosynthetic process	89	4	0.81	0.009
O-females						
1	GO:0022900	electron transport chain	36	6	0.22	4.9e-5
2	GO:0042773	ATP synthesis coupled electron transport	23	3	0.14	3.5e-4
3	GO:0055114	oxidation-reduction process	836	16	5.11	0.009

bioRxiv preprint doi: https://doi.org/10.1101/714048; this version posted July 24, 2019. The copyright holder for this preprint (which was not certified by peer review) is the author/funder, who has granted bioRxiv a license to display the preprint in perpetuity. It is made available under aCC-BY-NC-ND 4.0 International license.

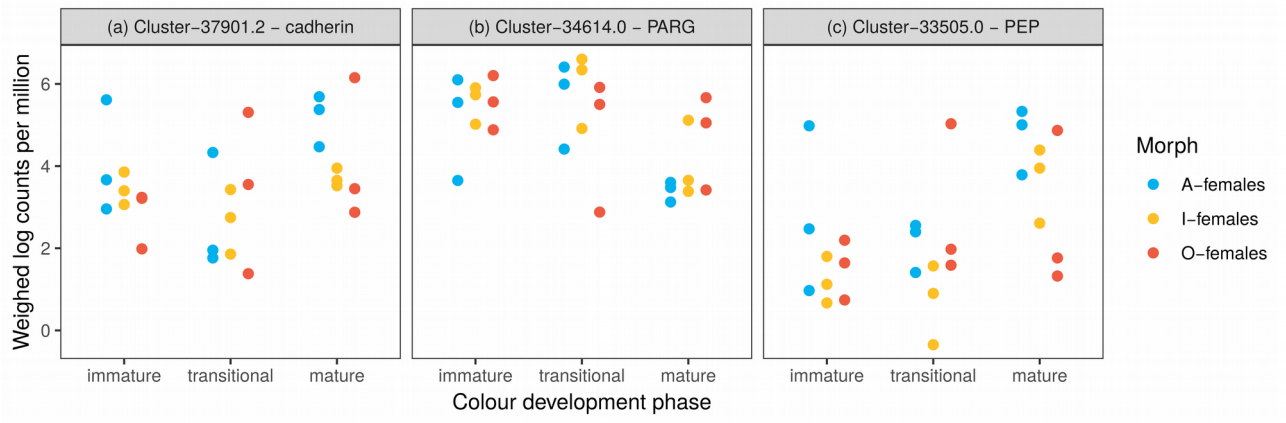

Figure S4. Expression pattern of genes co-regulated and potentially in epistasis (see Discussion) with a heterogeneous ribonucleoprotein during adult development of *I. elegans* females. Transcripts were annotated against the non-redundant database of the National Center for Biotechnology Information (NCBI). Expression data (log counts per million) have been weighed by within-sample variability and by the mean-variance relationship among genes, using 'voom' (see Methods).

bioRxiv preprint doi: https://doi.org/10.1101/714048; this version posted July 24, 2019. The copyright holder for this preprint (which was not certified by peer review) is the author/funder, who has granted bioRxiv a license to display the preprint in perpetuity. It is made available under aCC-BY-NC-ND 4.0 International license.

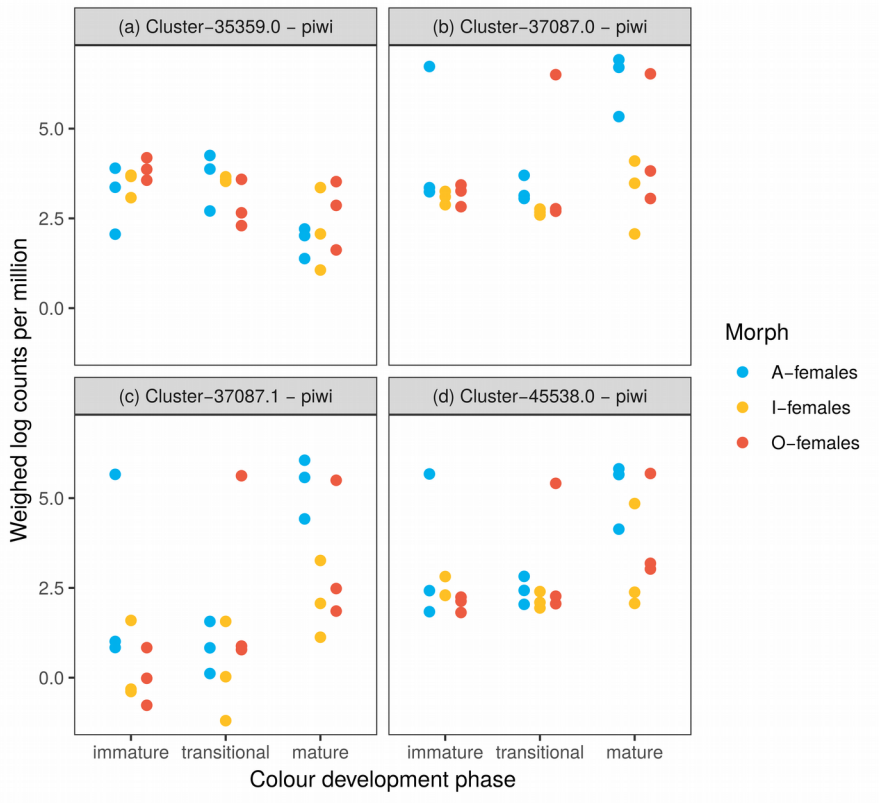

Figure S5. Expression patterns of genes in the *I. elegans* transcriptome with significant blast hits against piwi proteins in the non-redundant database of the National Center for Biotechnology Information (NCBI). Expression data (log counts per million) have been weighed by within-sample variability and by the mean-variance relationship among genes, using 'voom' (see Methods). Abbreviations: PARG = poly(ADP-ribose) glycohydrolase, PEP = protein on ecdysone puffs.

bioRxiv preprint doi: https://doi.org/10.1101/714048; this version posted July 24, 2019. The copyright holder for this preprint (which was not certified by peer review) is the author/funder, who has granted bioRxiv a license to display the preprint in perpetuity. It is made available under aCC-BY-NC-ND 4.0 International license.

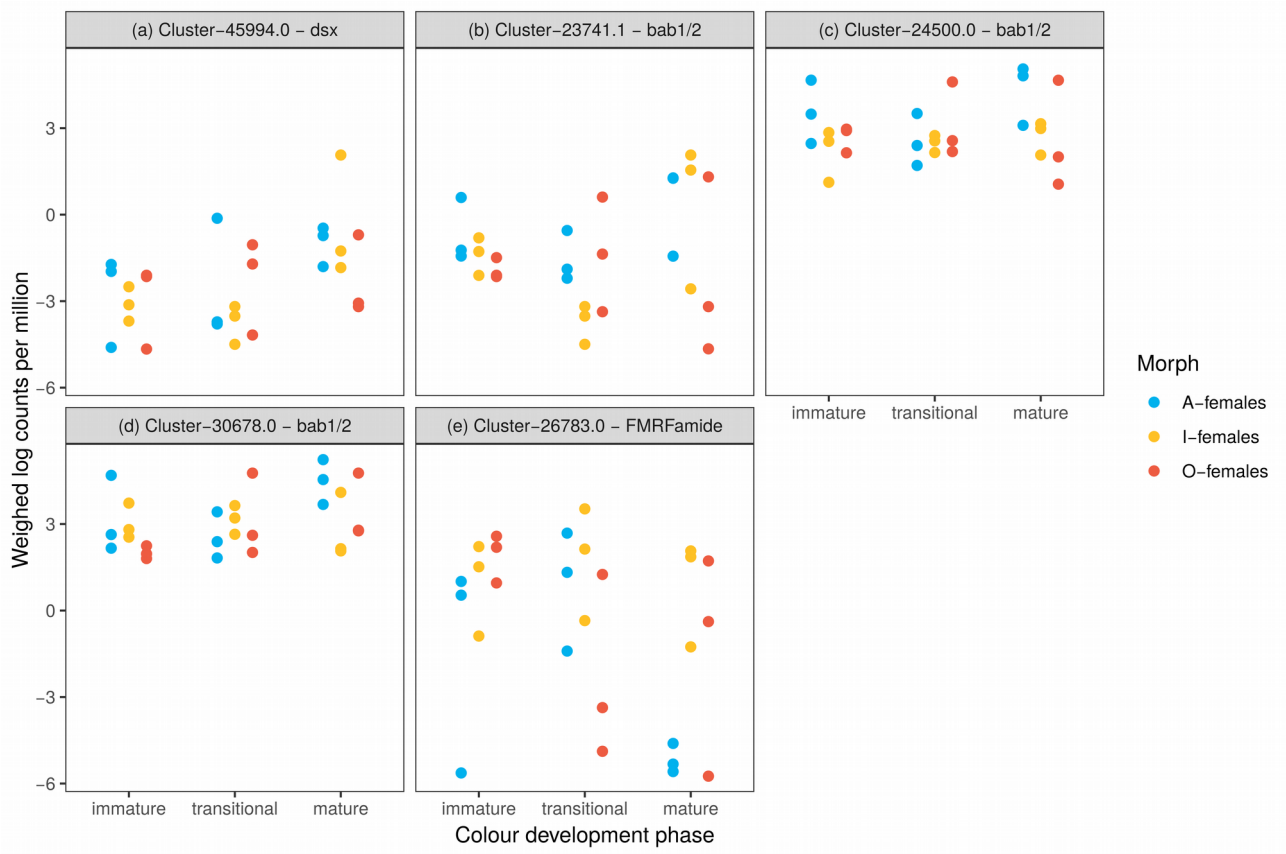

Figure S6. Expression patterns of genes in the *I. elegans* transcriptome with significant blast hits against *doublesex* (*dsx*) and two of its direct targets, bric-á-brac 1 and 2 (bab1/2) and FMRFamide, in *D. melanogaster*, in the non-redundant database of the National Center for Biotechnology Information (NCBI). Expression data (log counts per million) have been weighed by within-sample variability and by the mean-variance relationship among genes, using 'voom' (see Methods).